Co(II)-Imprinted Polymer Beads for Cationic Dye Removal from Water

Ezinne Favour Ogulewe

Submitted to the
Institute of Graduate Studies and Research
in partial fulfillment of the requirements for the degree of

Master of Science
in
Chemistry

Eastern Mediterranean University
September 2020
Gazimağusa, North Cyprus

Approval of the Institute of Graduate Studies and Research

Prof. Dr. Ali Hakan Ulusoy
Director

I certify that this thesis satisfies all the requirements as a thesis for the degree of Master of Science in Chemistry.

Prof. Dr. Izzet Sakalli
Chair, Department of Chemistry

We certify that we have read this thesis and that in our opinion it is fully adequate in scope and quality as a thesis for the degree of Master of Science in Chemistry.

Assoc. Prof. Dr. Akeem Oladipo
Co-Supervisor

Prof. Dr. Mustafa Gazi
Supervisor

Examining Committee

1. Prof. Dr. Mustafa Gazi

2. Prof. Dr. Osman Yilmaz

3. Asst. Prof. Dr. Ime Akanyeti

ABSTRACT

An adsorbent (Co(II)-imprinted polymer beads) was prepared using PVA/SA. The adsorbent was used to remove cationic dye (crystal violet) efficiently. Batch adsorption studies were performed in respect to variation in solution pH, dosage, initial dye concentration, contact time, temperature and binary system to check the effectiveness of the prepared beads in adsorbing CV. The adsorption kinetics, thermodynamics and isotherm were evaluated based on the parameters listed above. Structural characterization was done on the prepared and adsorbed beads using FTIR.

Maximum dye adsorption of 94 % was attained at pH 9, using 0.15 g adsorbent dose, at 90 min of contact time, with an initial CV concentration of 20 mg/L. Also the removal of CV is almost not affected by the presence of other cationic pollutants (methylene blue dye) in a binary system. The FTIR characterization revealed that CV was adsorbed onto the prepared adsorbent successfully and that the carboxyl group of the PVA/SA took part in the reaction.

The kinetic studies indicates that the adsorption process aligned with the pseudo-second-order kinetics. The thermodynamics parameters show that the adsorption process of CV onto Co-imprinted beads were exothermic, spontaneous and tends towards orderliness at low temperatures between 298 and 308 K. The ΔG value indicates a Physisorption process. The isotherm studies indicates that the adsorption mechanism is best explained by the Langmuir isotherm. The study has demonstrated that the prepared adsorbent (Co(II)-imprinted polymer beads) has a potential in adsorbing crystal violet dye from aqueous solutions.

Keywords: Co(II)-imprinted polymer beads; Crystal Violet dye; Adsorption studies; Adsorption kinetics; Isotherm studies

ÖZ

PVA / SA kullanılarak bir adsorbent malzem (Co (II) baskı polimer kürecikler) hazırlandı.Bu adsorbent, katyonik kristal Violet (CV) boyanın verimli bir şekilde adsorb edilmesinde kullanıldı. Hazırlanan küreciklerin CV adsorbsiyonundaki etkinliğini kontrol etmek için çözelti pH'ındaki, başlangıçtaki boya konsantrasyonundaki, temas süresindeki, dozajdaki, sıcaklıktaki ve ikili sistemdeki değişimleri incelemek için seri adsorpsiyon çalışmaları yapılmıştır. Adsorpsiyon kinetiği, termodinamik ve izotermler yukarıda listelenen parametrelere göre değerlendirildi. FTIR kullanılarak hazırlanan ve adsorbe edilen kürecikler üzerinde yapısal karakterizasyon yapıldı. Maksimum değer olan % 94 boya adsorpsiyonuna PH 9, 0.15 g adsorban dozu, 90 dakika temas süresi, 298 K ve 20 mg / L'lik bir başlangıç CV konsantrasyonuyla ulaşıldı. Ayrıca CV'nin adsorpsiyonunun, ikili bir sistemdeki diğer katyonik kirleticilerin varlığından neredeyse etkilenmediği saptandı. FTIR karakterizasyonu, CV'nin hazırlanan adsorbent üzerine başarıyla adsorbe edildiğini ve PVA / SA'nın karboksil grubunun reaksiyonda yer aldığını ortaya çıkardı. Kinetik çalışmalar, adsorpsiyon işleminin yalancı ikinci dereceden denklem ile tutarlı olduğunu göstermektedir. Termodinamik parametreler, CV'nin baskı kürecikler tarafından adsorpsiyon sürecinin ekzotermik olduğunu, kendiliğinden düzenli olma eğiliminde olduğunu ve 298 ile 308 K arasındaki düşük sıcaklıklarda verimli olduğunu göstermektedir. ΔG değeri, adsorpsiyon sürecinin fiziksel bir süreç olduğunu gösterdi. İzoterm çalışmaları, adsorpsiyon sürecinin en iyi Langmuir izotermiyle açıklandığını göstermektedir. Bu çalışma, hazırlanan malzemenin (Co (II) baskı polimer kürecikler) kristal violet boyanın sulu çözeltiden uzaklaştırılmasında absorbent malzeme olarak kullanılma potansiyeline sahip olduğunu göstermiştir.

Anahtar Kelimeler: Co (II) baskı polimer kürecikleri; Kristal violet boya; Adsorpsiyon çalışmaları; Adsorpsiyon kinetiği; İzoterm çalışmaları

DEDICATION

To my ever loving father Mr. Anthony Ifeanyichukwu Ogulewe.

ACKNOWLEDGMENT

My heartfelt gratitude to Assoc. Prof. Dr. Akeem Adeyemi Oladipo and Professor Mustapha Gazi their advice, lessons, guidance, support and detailed supervision through the course of this work.

My deepest appreciation to my lectures Professor Elvan Yilmaz and Professor Osman Yilmaz for impacting knowledge which was very useful and applicable in the course of this research.

I am grateful to my colleagues Ishaku Hamidu Bingong, Faisal Mustapha and Cahit for their assistance and support in the course of study.

My profound gratitude to my friends, Toochukwu Nnaji, Abdulhafiz Osuwa, Alpha Sumareh and Aderinshola Sontan for their tireless support and encouragement.

TABLE OF CONTENTS

LIST OF TABLES

LIST OF FIGURES

Chapter 1

INTRODUCTION

1.1 Water pollution

Water pollution remains a predominant issue that affects the world generally. In a long period, different types of pollutants and contaminants are continually released into the environment (water) by factories, pharmaceuticals, agriculture, mining sites, industries, etc. Groundwater and surface water are constantly polluted with aromatic hydrocarbons (PAHs), heavy metals, inorganic and organic chemicals, dyes and pesticides. These contaminants are dangerous and can, of course, cause permanent harm to the marine ecosystem and, in particular, to humans due to bioaccumulation and high rates of toxicity. (Huang et al., 2014). Hence, treatment of wastewater is very crucial before discharge into the environment and the pollutants should be minimized to the standard limit in compliance to water quality (Parlayici, 2019).

Different techniques have been employed to remove contaminants and pollutants present in wastewater. These methods include sedimentation, physical adsorption, filtration, coagulation, oxidation, biological methods and many others. However, most of these treatment techniques may not be completely effective for the removal of tiny sized and concentrated pollutants like endocrine-disrupting compounds (EDCs). Also, some of these methods may be efficient in the simultaneous removal of numerous pollutants but may not be effective in completely removing certain pollutants in wastewater (Huang et al., 2014).

Nevertheless, the adsorption technique has been reported as the most efficient in removing pollutants, most especially dye substances.

Lately, the application of biomaterials for the removal of pollutants is of rising interest due to their eco-friendliness, technical feasibility and reduction in cost compared to most other treatment techniques. Most especially is the use of biomaterials like natural polymers (Chen et al., 2010). Also, combining two or more polymers (biopolymers) are increasingly employed to enhance the cost performance of adsorbents (Zhu et al., 2012).

1.2 Background of the study

Dyes are increasingly used in the plastic, paper, cosmetic, ceramic, leather, printing, rubber, pharmaceuticals and textile industries to beautify their products. Also is the use of dyes in food, agriculture, photo-electrochemical cells and research industries. In fact, annually, an approximate of more than 700,000 tons of dye material is produced with over 100,000 variants in the market (Brillas & Martínez-Huitle, 2015). In the process of colouring, a good quantity of dye is absorbed on the product, while the other percentage ends up as industrial effluents (Fabryanty et al., 2017). During production, an estimate of twelve-hundredth part of synthetic dyes are lost and about twenty-hundredth part of this amount of spilled dyes find their way into the waste water of factories (Chakraborty et al., 2011). Dyes are a major source of water pollution that continue to pose serious threats to our ecosystem, due to its carcinogenic and toxic nature (Shoukat et al., 2017).

Figure 1.1: Dye polluted water.

Solving the problem of water pollution caused by dyes is of crucial importance to researchers and humans. These pollutants are particularly known to be very problematic as they affect the aesthetic nature of water and also prevents reuse (Brillas & Martínez-Huitle, 2015). A good number of these dyes generate mutagenic and toxic components when degraded which consequently have detrimental effects on aquatic organism. Biochemical process in water polluted with dyes may be halted due to reduced light penetration caused mutagenic compounds formed from the degradation of dyes (Oladipo & Gazi, 2015).

Different methods have been used to treat polluted water containing dyes. These techniques include electrocoagulation, photo-degradation and biochemical degradation. Most of these treatments are time-consuming, require efficient purification, and are complicated and expensive. However, the adsorption method is

preferable owing to its efficiency, regeneration ability, simplicity, potential to remove a tiny quantity of dye and low cost. Low-cost adsorbents include activated carbon, saw dust, papaya seed, banana and orange peel which have displayed a high adsorption capacity and are abundant and ecofriendly (Oladipo & Gazi, 2015).

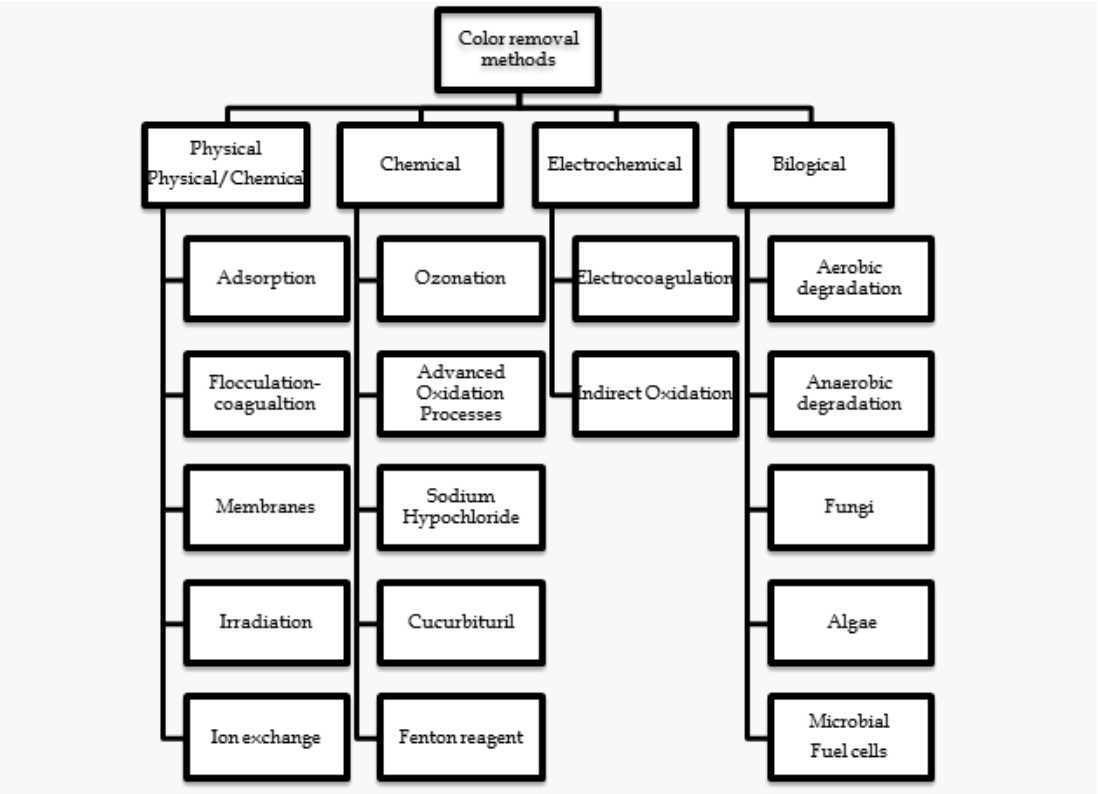

Figure 1.2: Dye removal methods from effluents (D'Antoni et al., 2017).

1.3 Aim and objectives of the study

This study aims to synthesize, characterize and explore the potential of cobalt imprinted polymer beads (adsorbent) for the removal of cationic dye (crystal violet) from aqueous solutions.

The objectives include:

1. To develop cost-competitive cobalt imprinted polymer beads for treating crystal violet dye polluted water.

2. To investigate the performance of cobalt imprinted polymer beads under variation of influencing parameters like contact time dosage, solution pH and temperature on dye adsorption.
3. To establish the governing thermodynamics, isotherms and adsorption kinetics during the adsorption process.

1.4 Significance of research

1. Results from the research will provide a simple and new process in preparing cost-competitive adsorbents for water treatment; especially dye polluted water.
2. Results herein will be useful in updating the latest advances in water treatment using cobalt imprinted polymers-based adsorbents.

1.5 Scope of the study

The study will cover the synthesis and application of cobalt imprinted polymer beads for treating dye (crystal violet) polluted water. The mechanism of the adsorption will be established in detail via thermodynamic, isotherm and kinetic data.

It is worth mentioning that, the characterization of the cobalt imprinted polymer beads is limited to only Fourier-transform infrared spectroscopy (FTIR) technique due to the lack of facility and current virus pandemic to explore other facilities outside the university.

Chapter 2

LITERATURE REVIEW

2.1 Dye water pollution

Dye polluted water is very detrimental to mankind and the environment we live in due to the deadly disease they might induce on humans and aquatic organism. Dyes also destroy the esthetic nature of water, which may bring about a reduction of aquatic life. Most dyes have a very large structural composition which makes them very challenging to decolourize and toxic even in small quantity (less than 1ppm) (Hamidzadeh et al., 2015). Its increased toxicity is caused by a series reaction like oxidation and hydrolysis of dye (An et al., 2014).

Besides, their resistance to aerobic digestion, natural degradation, photo-stability, oxidation and their ceaseless colour prevents the passage of sunlight into the water, therefore depleting dissolved oxygen and thereby destroys aquatic life. The complicated chemical structure of most dyes makes them very recalcitrant and resistant to biological, physical and chemical treatment (Kulkarni et al., 2017). Among the classes of dyes, cationic are known to be very toxic as they pollute the ecosystem as well as contaminate the food chain by influencing it with harmful toxins (Rai et al., 2015). Hence, the treatment of dye polluted water of the utmost interest and importance to researchers and environmentalist (Oladipo & Gazi, 2014).

A lot of methods have been devised to treat dyes in wastewater. Among the techniques include biological treatment which entails the use of microorganisms, bacteria, enzymes and activated sludge; physiochemical treatment which entails reverse osmosis, flocculation/coagulation, ozonation and oxidation; physical treatment which entails ion exchange, membrane filtration, adsorption and electrochemical techniques (Fabryanty et al., 2017). However, adsorption has proven to be outstanding due to its flexibility, low cost and efficiency which is also highly dependent on the type of adsorbent used. Several adsorbents, like zeolites, active carbon and natural materials (sawdust, papaya seed, banana and orange peel) (An et al., 2014), and the by-products of the olive oil industry have been applied to treat organic dyes (Rai et al., 2015).

Nevertheless, activated carbon powder has been commonly used and is known to be the most flexible adsorbent for water pollution management owing to its thermal stability, large surface area as well as the porosity. Even then, as the activated carbon material is depleted, problems exist in the extraction and recycling of activated carbon. Isolation of activated carbon usually requires procedures like centrifugation or filtration, which may lead to the loss of activated carbon or the obstruction of filters. Pollutant-charged activated carbon obtained from effluent treatment contributes to second-rate pollution (Rai et al., 2015). Nevertheless, the problems can be eliminated by modifying activated carbon with organic or inorganic compounds, most especially is the use of magnetic compounds like iron oxide as reported by Hamidazadeh et al. for the adsorption of crystal violet. Magnetic compounds are reported to have an increased rate of separation (Hamidzadeh et al., 2015). Besides, producing activated carbon from biomaterials are inexpensive in comparison to its commercial counterpart. Recently too, waste biomaterials like orange peel, rice hulls, oil palm shells, coconut husk have been used to produce activated carbon (Aljeboree et al., 2017).

2.2 Dyes

Dyes are generally classified into natural and synthetic dyes. Natural dyes are known to originate from natural sources like animals, plants and minerals. These dyes are used together with metallic salts like mordant for enhanced colouring of material. Different synthetic dyes are majorly used by the fabric industries to enhance the quality of their product (Benkhaya et al., 2018). Dyes are also classified according to their chromophore, name and characteristic property (Brillas & Martínez-Huitle, 2015).

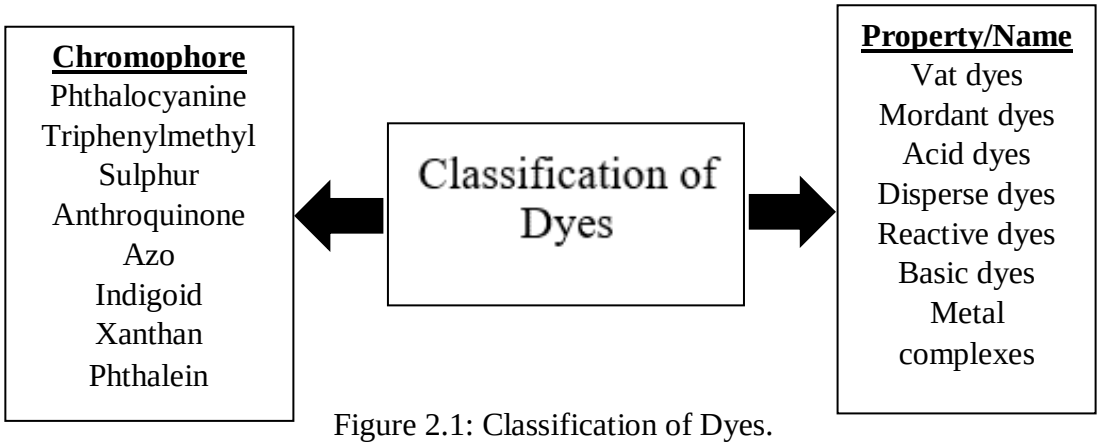

Figure 2.1: Classification of Dyes.

Among these classes of dye, the azo dyes, vat dyes and reactive dyes are mostly used to print dye fibres of cotton. Acid dyes are negatively charged dyes that are applied under acidic pH medium. These dyes are characterized by one or multi acidic functional groups. They are mostly used on wool, cotton, nylons etc. Examples are acid blue and acid orange (Benkhaya et al., 2020).

Disperse dyes are extensively used to dye acetates and polyesters. They are known for being water-insoluble, but soluble in fibre. This property makes it difficult to extract them after they have been used on materials. Reactive dyes are known to have a great

colour fastness due to constant covalent bonds. They are mostly used on cellulose, silk and wool fibres (Sikaily et al., 2012).

Azo dyes have been the most extensively used dyes most especially in the clothing industries. They are characterized by excellent colour fastness, colour strength, bright shades etc. Basic dyes otherwise called cationic dyes are soluble in water and give cations when in aqueous solution. Their positive charge is distributed as a delocalized charge around the dye cation just like xanthenes, triarylmethyl and aridine dyes. The positive charge could also be localized on an ammonium group. These dyes are mostly used on papers, acrylics, polyester and nylon materials (Benkhaya et al., 2018). A typical example is the crystal violet dye, which will be discussed in the next section.

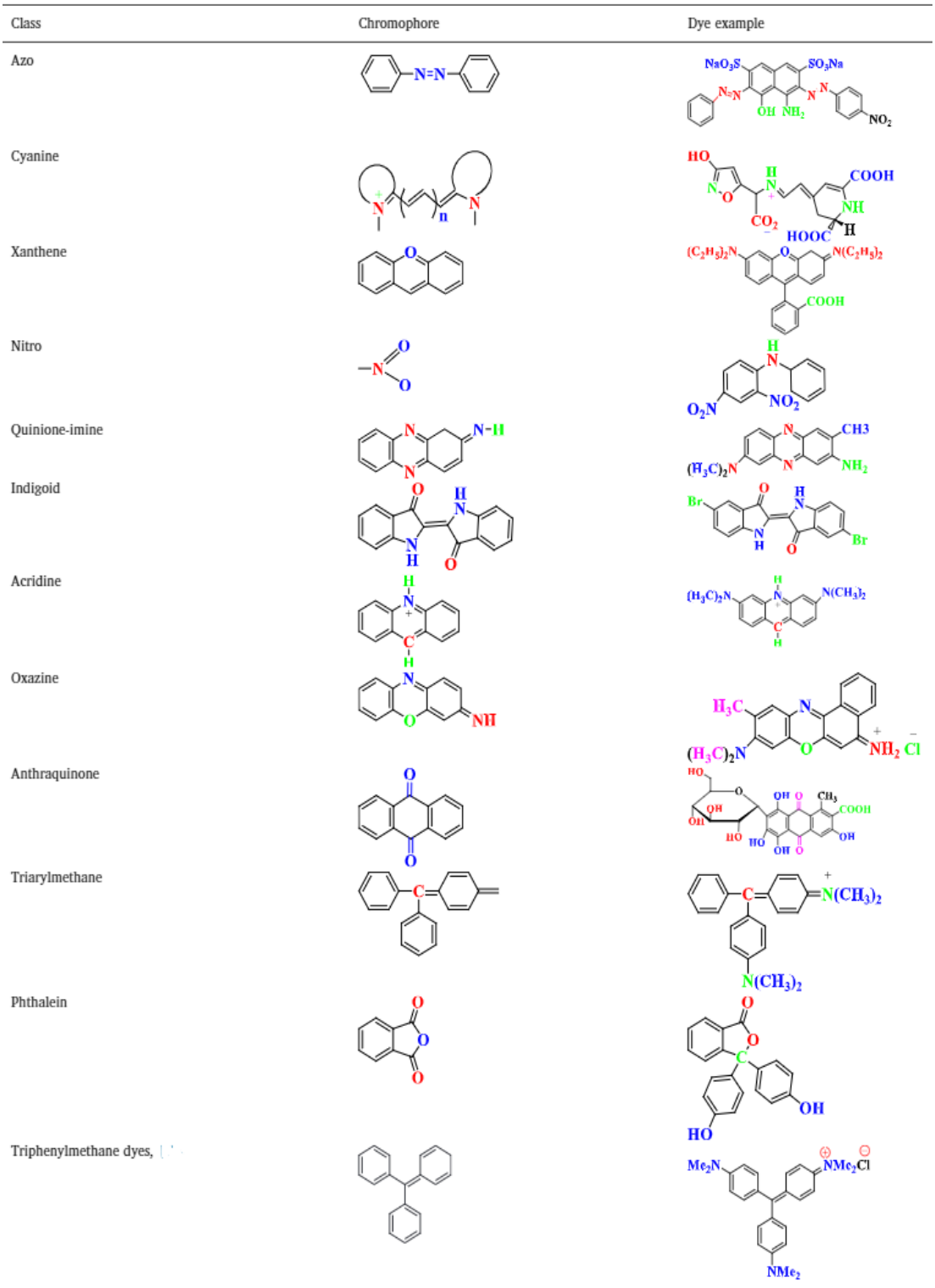

Figure 2.2: Common classes of dye by their chromophore (Benkhaya et al., 2020).

2.2.1 Crystal violet (CV)

Crystal violet otherwise called hexamethyl pararosaniline chloride is a basic synthetic cationic dye that is widely used and can be classified among the triphenylmethane class

of dyes. They are used as skin disinfectant, bacteriostat and histological stain in the medical field, supplement to poultry feed to inhibit mold propagation and intestinal parasite (Hamidzadeh et al., 2015; Oladipo & Gazi, 2014). It has commonly been used in the textile industry as a purple dye to dye silk, wool and cotton, also in the production ink and paint. Besides, as a protein pigment, is used as a "booster for bloody fingerprints" (Chakraborty et al., 2011). They find their way into the water bodies from the effluents of numerous industries especially the paint, textile, biotechnology and medical industries. Crystal violet dye, even at a concentration of less than 1ppb is considered to be teratogenic, poisonous and mutagenic to animals as well as humans (Kulkarni et al., 2017).

When inhaled or consumed, crystal violet can be dangerous and may lead to loss of eyesight, skin irritation, nausea, excessive sweating, hypermotility, abdominal pain, irreversible eye/cornea damage, difficult breathing (Fabryanty et al., 2017). All these detrimental effects of crystal violet call for its removal from industrial wastewater before releasing it into the environment (Hamidzadeh et al., 2015; Oladipo & Gazi, 2014).

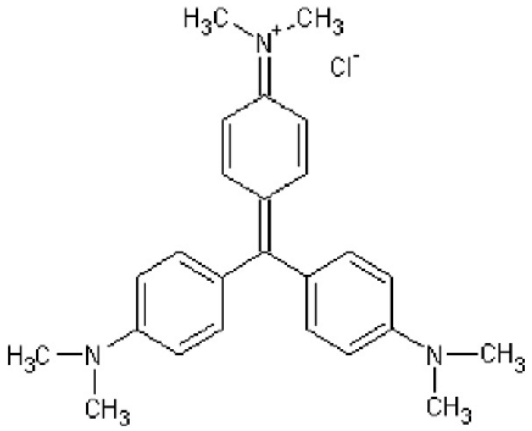

Figure 2.3: Crystal Violet structure.

2.3 Adsorption process

Adsorption is a process that involves the transfer and aggregation of compounds/substances at the interphase of either a liquid/solid, liquid/liquid interphase etc (De Gisi et al., 2016). The absorbing substance is called **adsorbent**, while **adsorbate** is the entity that is adsorbed. The chemical and physical properties of an adsorbent determine its effectiveness. The physical characteristics include the surface area and the pore size which determines the reachability and interactivity between the adsorbate and the adsorbent. While, the chemical characteristics which are predominantly the functional groups influence desorption ability and the kind of adsorption force (Li et al., 2019). The adsorption method in the solid-liquid form includes the elimination and deposition of solutes from the solid-phase solution. A stable equilibrium is achieved between the solute left in the aqueous solution and the solute adsorbed on the solid surface (De Gisi et al., 2016). There are two main adsorption processes namely chemisorption and physisorption processes and are discussed below.

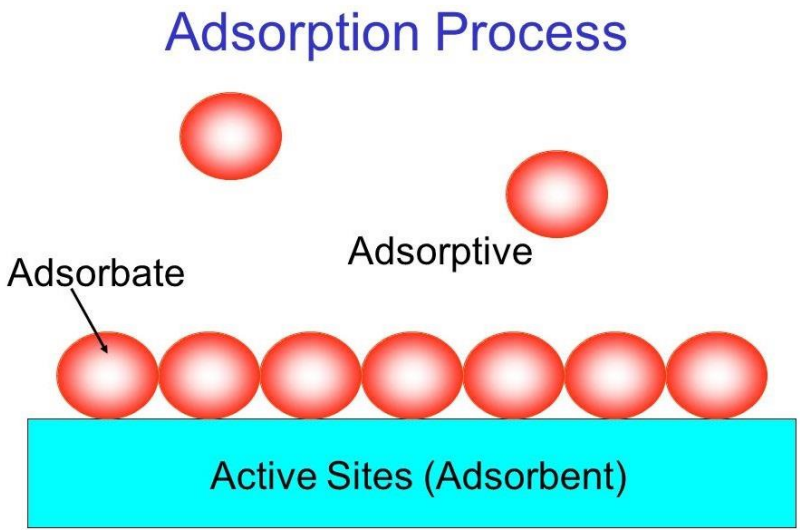

Figure 2.4: Adsorption process (https://slideplayer.com/slide/1525531/).

2.3.1 Physisorption

Involves the physical interaction between the solid surface and the adsorbed particles. This process occurs below the critical temperature of the molecule adsorbed and is reversible because the attraction interactions are van der Waals force and are weak. This system is exothermic as it entails a decrement in entropy and free energy of the adsorption process.

2.3.2 Chemisorption

Involves the chemical interaction/bonding between the solid surface and the substance adsorbed. The attraction forces here are stronger. These two interactions may occur independently or simultaneously (De Gisi et al., 2016).

Inexpensive adsorbents such as clay, zeolite, lignin, chitosan, alginate etc., have been used for removing pollutants and contaminants (Huang & Wang, 2018).

Table 2.1: Difference between Chemisorption and Physisorption

Properties	Chemisorption	Physisorption
Force of adsorption	The chelating formation, ion exchange and electrostatic attraction.	Hydrogen-bond interaction and Vander Waals force,
Heat of adsorption	80,000-400,000 J/mol	Less than 40 mJ/mol
Rate of adsorption	Often time-consuming	Rapid
Temperature	High	Low
Number of the adsorption layer	Monolayer	Monolayer/multiple layers

Selectivity	Yes	No
Adsorption-desorption process	Irreversible	Reversible

(Liu et al., 2019).

2.4 Factors affecting adsorption

2.4.1 Chemical and physical characteristics of adsorbents

Adsorption is practically a surface phenomenon. Hence, higher adsorption occurs when the adsorbent has a greater specific surface area. Surface area and distribution pore structure and particle size vary with different preparation methods and types adsorbates. Also, the surface charge properties and surface chemical structure of adsorbents affect adsorption process (Liu et al., 2019).

2.4.2 Concentration of adsorbate

The molecular size and dissolution of adsorbate have a notable effect on the adsorption rate and efficiency. The diffusion coefficient and adsorption rate increases with smaller molecular volumes of adsorbates. Adsorption capacity is optimized by increasing the concentration of adsorbate (Liu et al., 2019). Kulkarni et al reported a decline in the quantity of crystal violet dye adsorbed per-unit weight of adsorbents (water hyacinth) as the concentration of crystal violet dye was increased in their study. The trend was attributed to an increased surface activity of adsorbate (Kulkarni et al., 2017). A decrease in the adsorption capacity was observed with an increment in the initial concentration of methylene blue. Adsorption efficiency decreased from 100 % at 100 mg/L to 55 % at 2200 mg/L in a study by Lin et al. The trend was attributed to excess active sites at lower concentrations of methylene blue, whereas the steady active sites

could not bind the increasing molecules of MB at higher concentrations (Lin et al., 2020).

2.4.3 Temperature

For chemisorption, higher temperature favours adsorption process, while a lower temperature favours physisorption (Liu et al., 2019). As reported by Aljeboree et al. in their study on the adsorption of direct yellow and maxilon blue dye onto activated carbon based on coconut shells as adsorbent, the percentage of adsorption declined with an increase in temperature from 10 – 40 ^{o}C, which indicated that the adsorption process was exothermic. This was attributed to the Brownian motion of molecules and increased solubility of dye molecules which led to a subsequent stronger bonding between the solvent and the dye molecules than between the adsorbent and dye molecules. They also pointed out that the breaking of hydrogen bonds in the dye compounds at high temperature contributes to the behaviour and adsorption process (Aljeboree et al., 2017). Also reported by Oladipo and Gazi, in their study of the enhanced removal of CV using alginate/acid bentonite composite as adsorbent, the percentage adsorption increased as the temperature increased, which implied that the adsorption process was endothermic. The trend was attributed to initiation of the adsorbent surface and expansion of pores, which subsequently led to an improvement in the rate of diffusion of CV dye within the pores and across the outer layer (Oladipo & Gazi, 2014).

2.4.4 Contact time

Adsorption capacity increases as the contact time between adsorbents and adsorbates increases until an equilibrium adsorption point is attained. Hence, adsorption efficiency and rate is significantly dependent on the time taken to reach an equilibrium point. Besides, equilibrium might be reached in a short time if the adsorption rate is

fast (Liu et al., 2019). In a study by Shoukat et al. on the removal of CV using mango stone biocomposite, they observed very fast adsorption and then slow adsorption after equilibrium at a contact time of 30 min. This result meant that the bio-composite prepared by Shoukat was very efficient for the removal of CV since equilibrium was attained in a rapid short phase of 30 min. The fast adsorption before equilibrium was as a result of free binding sites. Meanwhile, the slow adsorption could be due to the depletion of free active sites and electrostatic repulsion between the dye ion and already adsorbed ions (Shoukat et al., 2017). Lin et al. in their study on the adsorption of methylene blue by waste black tea powder reported an increment in the percentage removal with an increase in contact time. In the first 20 min, the adsorption efficiency was said to have increased rapidly, whereas between 60 to 120 min contact time, a slow increase in the adsorption efficiency was observed (Lin et al., 2020).

2.4.5 Solution pH

pH value is a very crucial parameter to be considered in adsorption studies, because it strongly influences the surface properties of adsorbents and ionization/dissociation of adsorbate (Oladipo & Gazi, 2014). Highly basic solutions are inappropriate for most adsorbates, most especially heavy metals because they tend to precipitate in this medium, as well as highly acidic conditions, in which the protons in the medium compete with ions from the adsorbates (Liu et al., 2019). For example, in a study reported by Oladipo & Gazi on the enhanced adsorption of crystal violet dye onto alginate/acid-activated bentonite composite beads. Adsorption of crystal violet dye increased significantly with a high pH range between pH 8 and 10. This was due to the electrostatic interaction (attraction) between the negatively charged adsorption sites of the adsorbents and the positively charged dye (CV) molecules (Oladipo & Gazi, 2014). Also, in a study reported by Fabryanty et al. on the enhanced adsorption of crystal

violet dye onto bentonite/alginate composite. The adsorption of crystal violet dye increased significantly with an increase in pH between 3 and 9. High percentage removal of about 98 % was recorded at pH 6. This was ascribed to the electrostatic attraction between the negatively charged adsorption sites of the adsorbents and the positively charged dye (CV) molecules (Fabryanty et al., 2017). Also, Kulkani et al. reported an increase in the percentage removal of CV using water hyacinth as they increased the pH of the CV. They reported the highest percentage of removal at pH 7.8 (Kulkarni et al., 2017). Al-Senani and Al-Kadhi observed a decrease in the adsorption of fluorescein dye with an increment in the pH from 6 to 12. The trend was ascribed to the adsorption of hydroxyl ions on the surface of the adsorbent there making it negatively charged (Al-Senani & Al-Kadhi, 2020).

2.4.6 Presence of interfering substance

In the physisorption process, adsorbents may adsorb a range of adsorbates in solution. However, if the adsorbates in solution are at the same concentration, the adsorption capacity might decrease for one of the adsorbates. This is because, the solutes in solution will compete of active sites for adsorption (Liu et al., 2019). In a study by An et al the influence of common salt (NaCl) was investigated on the removal of crystal violet and congo red using magnetic calcium ferrite nanoparticle as adsorbent and 0.02 M and 0.2 M of the salt. They reported that the salt did not influence the adsorption efficiency of crystal violet and/or congo red (An et al., 2014). Guo et al., observed that the presence salts like KCl affected the adsorption capacity of rhodamine B using porous carbon-based on rice husk as adsorbent. An increase in the concentration of KCl resulted to an increment in the adsorption capacity of rhodamine B while smaller concentrations affects the adsorption capacity slightly (Guo et al., 2005). Mohanty et al. also reported a decline in the degradation efficiency of CV in the presence of

calcium, nitrate, sulphate and chloride anions with varying concentrations between 50 to 400 mg/L. This behavior was ascribed to the ability of the ions of each salt to coat on the adsorbent titanate nanotube thereby leading to hindrance in the transfer of electrons (Mohanty et al., 2020).

2.4.7 Dosage of Adsorbent

In a study involving the adsorption of CV using water hyacinth, Kulkarni et al. reported a notable increase in the percentage removal of crystal violet from 73.48 % to 90 % with an increment in the dosage of the adsorbent (water hyacinth) from 500 mg to 1500 mg. It was further reported that the percentage remained constant with more increase in the dosage of the adsorbent. This was ascribed to the saturation of binding sites due to the accumulation of adsorbed particle (Kulkarni et al., 2017). Also, in a study by Mohanty et al. on the adsorption/photo-degradation of CV using titanate nanotube, noted that the percentage removal of CV increased as the adsorbent dose was increased from 1 g to 5 g. Up to 95 % percentage adsorption of CV was achieved after 6 h. The increase reported was attributed to an increase in active site precursors (Mohanty et al., 2020). Oladipo and Gazi also reported an increment in the percentage adsorption of CV by increasing the dosage of adsorbent in their study on the enhanced removal of CV using alginate/acid bentonite. This was ascribed to an enlarged surface area of adsorbent and the presence of extra active sites for adsorption (Oladipo & Gazi, 2014). In a study by Rapo et al. on the removal of remazol brilliant violet dye using eggshell, the removal efficiency of the dye was observed to increase with an increase in the adsorbent dosage from 500 mg to 2500 mg. Up to 94 % was obtained at 2500 mg of adsorbent dose (Rápó et al., 2020).

2.5 Adsorption Isotherm Models

Adsorption isotherm models are used to define the relationship between residual adsorbate in solution and the equilibrium mass of adsorbed adsorbate. The set of data used to establish this relationship are attained by conducting fixed adsorption in a batch process (Karimi & Tavakkoli, 2019). Identifying, interpreting and understanding the appropriate isotherm model is very vital for designing, modelling and improving an adsorption system (Ayawei et al., 2017). The parameter in this models could give information of the mechanism of adsorption, the surface property of the adsorbent, the degree of affinity between the adsorbent and adsorbate, and the extent of coverage of adsorption sites (Karimi & Tavakkoli, 2019).

A lot of isotherm models are listed in literature according to the number of empirical parameters, with one-parameter isotherm being the simplest of all, which is known as Henry's isotherm model which is subject to the proportionality between the amount of adsorbate surface and the partial pressure of the adsorptive gas (Ayawei et al., 2017).

The two-parameter isotherm models include among others the Hill-Deboer model, Flory-Huggins isotherm, Jovanovic isotherm, Fowler-Guggehein model, Halsey isotherm, Hill isotherm, , Kiselev isotherm, Harkin-Jura isotherm, Elovich isotherm. Besides are Langmuir isotherm, Temkin isotherm Freundlich isotherm and Dubinin-Radushkevich isotherms which are explained later.

Three-parameter isotherm includes Redlich-Peterson isotherm, Toth isotherm, Sips isotherm, Kahn isotherm, Koble-Carrigan isotherm, Radk-Prausniiz isotherm, Langmuir-Freundlich isotherm, Jossens isotherm etc. Four-parameter isotherm includes Weber-van Vliet isotherm, Baudu isotherm, Fritz-Schlunder isotherm,

Marczewski-Jaroniec isotherm. Lastly, is the five-parameter empirical isotherm which was developed by Schlunder and Fritz (Ayawei et al., 2017).

2.5.1 Langmuir Isotherm

This adsorption isotherm best explains the equilibrium between the adsorbent and adsorbate system. Here, adsorption is restricted to a monolayer before or at a unity value of relative pressure (Liu et al., 2019). The Langmuir model predicts that monolayer sorption takes place on the solid substrate with uniform sites and that once these sites are loaded up with dye molecules, adsorption discontinues (Aljeboree et al., 2017). This isotherm could be used to explain the chemisorption process and the mechanism of the binary adsorption system. Langmuir's model also proposes that desorption and adsorption rates are equal at equilibrium and that the fractional surface distribution is directly proportional to the surface desorption rates (Liu et al., 2019).

The filled-up monolayer isotherm is described by the equation below:

$$qe = \frac{q_{m\ b}C_e}{1+bC_e} \qquad (2.1)$$

where:

C_e = Concentration of adsorbate at equilibrium (mgL^{-1});

q_e = Adsorption capacity at equilibrium;

q_m = Maximum dye uptake (mg/g);

b = Constant denoting adsorption energy (Lmg^{-1}).

2.5.2 The Freundlich Isotherm

This adsorption isotherm which is an analytical method best explains the non-uniformity of heat distribution on the adsorbent surface, which also indicates that adsorption is heterogeneous (Aljeboree et al., 2017).

Freundlich equation as shown by the expression:

$$Q_e = K_f C_e^{1/n} \quad (2.2)$$

where:

n = Freundlich constants for adsorption intensity

K_F = Freundlich constants for adsorption capacity.

The degree of non-linearity between adsorption and solution concentration depends on the adsorption intensity (n) in the following ways:

i. The adsorption process is linear when the value of n approaches or equals unity.

ii. Adsorption is a chemical process when n value goes below unity.

iii. Adsorption is a physical process when the value of n goes above unity (Aljeboree et al., 2017).

2.5.3 Dubinin-Radushkevich (D-R) Isotherm Model

The Dubinin-Radushkevich (D-R) isotherm model assumes that the size of an adsorbent is similar to the micro-pore size and that the equilibrium adsorption in respect to a specific adsorbent-adsorbate mixture can be expressed alone without temperature by making use of the adsorption potential (ε) (Piccin et al., 2011).

$$\varepsilon = RT \ln \left[1 + \frac{1}{C_e}\right] \quad (2.3)$$

The D-R isotherm implies the distribution of the response curve by Gaussian-type and the formula can be defined by the equation below:

$$\text{Ln } q_e = \ln q_s - B\varepsilon^2 \quad (2.4)$$

where:

q_s = Constant of D-R ($molg^{-1}$)

B = mean adsorption free energy E (kJ/mol) per adsorbate molecule at the time of transition from the bulk solution to the solid surface which is represented by the equation below:

$$E = \frac{1}{(2B)^{\frac{1}{2}}} \quad (2.5)$$

q_s and B values can be obtained through a linear approximation of the D-R isotherm. A plot of ln qe against ε using equation (2.4) gives a straight-line graph with the slope as B and intercept ln(q_s) (Piccin et al., 2011).

2.5.4 Temkin isotherm

This model suggests that at maximum energy levels, adsorption is depicted by a homogenous dispersion of binding energies and that an increase in the surface area of the adsorbent leads to a decrease in the energy of adsorption of all molecules.

The Temkin isotherm is explained by the equation below:

$$q_e = \frac{RT}{b} lnK_T + \frac{RT}{b} lnC_e \quad (2.6)$$

where:

K_T = Equilibrium constant ($Lmol^{-1}$)

b = Adsorption heat

R = Universal gas constant (8.314 J $K^{-1}mol^{-1}$)

T = Temperature (K).

A plot of q_e versus ln(Ce) using equation (2.6) gives a straight line graph of intercept (RT lnK_T)/b and slope RT/b (Piccin et al., 2011).

2.5.5 Redlich-Peterson (R-P) isotherm

The Redlich-Peterson (R-P) isotherm model is a very versatile model, which may be applied to either heterogeneous or homogenous systems. It describes adsorption equilibrium over a broad concentration. The equation below represents the model.

$$\ln\left[K_R \frac{C_e}{q_e} - 1\right] = ln(a_R) + \beta ln(C_e) \quad (2.7)$$

where:

K_R = R-P constant (Lg^{-1}),

a_R = R-P constant (Lmg^{-1})

β = exponent which lies between 1 and 0.

Plotting a graph of the left side of the equation (2.7) against ln Ce to achieve the isotherm constants is not valid because of the three unknowns, β, a_R and K_R. Nevertheless, the method of optimizing the coefficient of correlation is then used to solve equation (2.7) by reducing the difference between theoretical model projections and the experimental data points (Piccin et al., 2011).

2.6 Adsorbents

Different materials have been used as adsorbents in literature. Activated charcoal, for its simplicity, high adsorption capacity and surface area have been termed a universal adsorbent as it has been used to remove a lot of pollutants from solution (Yadav et al., 2020). Adsorbents such as alginate/natural bentonite composite beads, calcium alginate/acid-activated organobentonite composite beads, natural clay of Agadir region, graphene oxide intercalated montmorillonite nanocomposites, sodium alginate-based inorganic/organic superabsorbent composite, magnetic calcium alginate beads chitin/clay microspheres, zeolite nanostructures, chitosan/cellulose beads, have been used to remove dye substances from wastewaters (Parlayici, 2019).

Other adsorbents include functionalized graphene oxide, activated carbons, zeolites, red mud, agricultural wastes, polymers like kappa-carrageenan/PVA nanocomposite hydrogels, polyvinyl alcohol aerogels based on activated carbon,

polyacrylonitrile/TiO_2/PVA and cryogel beads based on graphene oxide-alginate have all been employed for the adsorption of methylene blue in industrial sewage (Yadav et al., 2020).

Alginate coated perile beads were synthesized by Parlayici and utilized for the adsorption of malachite green, methyl blue and methyl violet at pH 6. Alginate coating was proven to be efficient for enhancing the adsorption capacity of MG, MV and MB (Parlayici, 2019). Sen et al. also prepared a polymer composite made up of polyethylene and green clay for the efficient removal of methylene blue at a pH of 9. It was reported that the prepared composites separated methylene blue from water readily (Şen et al., 2018).

2.7 Molecular Imprinted Polymers

Most lately, molecularly imprinted polymers (MIPs) and ion are of increasing interest due to their outstanding selectivity. Molecularly imprinted polymers (MIPs) are synthesized polymers that have the advantage of maintaining distinct cavities fashioned for specific molecules. MIPs are synthesized by copolymerizing a crosslinking agent with an already prepared complex. This complex could be prepared from a monomer and template with functional groups particularly bonding with the template by non-covalent or covalent bonds. The consequent disposal of the imprint template creates unique cavities whose functional group, structure and size are analogous to the molecular template (Huang et al., 2014). A tailored binding pocket and the prearranged ligand is left after the template molecules has been disposed. Thus, this imprinted polymer reveals the resemblance of the template molecule to certain structurally similar compounds. (Saraji & Yousefi, 2009).

This purposed selectivity makes molecularly imprinted polymers (MIPs) an excellent material for wastewater treatment (Huang et al., 2014). For metal ions, the term ionic imprinting is used rather than molecular imprinting. Molecularly imprinted polymers (MIPs) are similar to ion-imprinted polymers (IIPs), only that after imprinting (IIPs) identify inorganic ions (Saraji & Yousefi, 2009). In general, ion imprinted polymers are synthesized by forming an enhanced and stable cross-linked substance on the basis of a metal ion.

Ion imprinted polymers can be prepared by suspension, bulk and precipitation polymerization. The functional monomers form coordinate complexes with metals and ligands, due to a more stable and stronger bond interaction. Also, by regulating the experimental conditions, the speed of breaking and binding cohesion bonds can be adjusted. Chelation of metal ion is known to have a higher accuracy than covalent bond chelation and is stronger than electrostatic bonding and hydrogen bonding (Liu et al., 2020).

The metals ions of an ion imprinted polymers participate in the binding phase of adsorption first and then the imprinting phase takes place once the metal ions can be sensed upon cavity formation. They are as well similar to molecularly imprinted polymers (Biswas et al., 2019). Latest findings have shown that IIPs are promising for adsorbents especially metal ions. Ion imprinting is a simple and reliable separation technique for the quick synthesis of organic and inorganic polymeric materials that bond the template ion selectively. Conversely, most conventional imprinting approaches have certain drawbacks that include reduced hydrophilicity, since a good number of the imprinted sites are prepared from functional monomers of lower attraction to water in carbon-based solvent conditions. Conventional ion printing

technologies are based on 3D polymer networks and the templates are inserted deep within the polymer matrices. The surface ion printing technique can solve these disadvantages due to the complete elimination of the templates and strong accessibility to the target material (Kang et al., 2016).

2.8 Polyvinyl alcohol (PVA)

Polyvinyl alcohol (PVA) is a synthetic polymer with a good amount of –OH functional groups. It has excellent properties of being chemically stable, biocompatible, non-toxic, biodegradable, is inexpensive, simple to prepare, and has an appealing mechanical property. This property has made it very useful for biomaterial applications (Zhu et al., 2012; Zhu et al., 2014). Despite all of these, PVA used on its own has a drawback of absorbing pollutants and contaminants at a low rate.

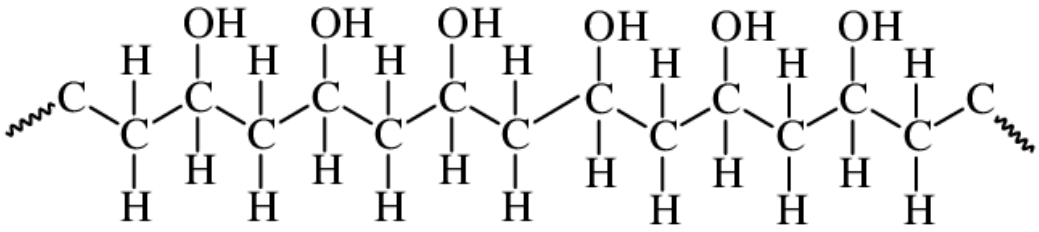

Figure 2.5: Chemical structure of polyvinyl alcohol (PVA).

2.9 Sodium Alginate (SA)

Sodium alginate is a linear natural polymer that is derived from sea brown algae/seaweed of the Phaeophyceae family. It is an anionic polysaccharide made up of two distinct monomeric units: (1,4-linked) α-l-guluronate (G) and β-d-mannuronate (M), arranged in blocks of M-G, G-G and M-M. Sodium alginate has an excellent property of reacting efficiently with hydrogen and carbonyl group and a great formation of a membrane (Chen et al., 2010; Mallepally et al., 2013; Yue et al., 2016). The presence of the hydroxyl (−OH) groups and carboxyl groups (−COOH) as reaction

and coordination sites on the backbone of SA makes it a very efficient adsorbent for the removal of water contaminants and pollutants like metal ions, microorganisms, fertilizers, dyes and enzymes. This carboxyl and hydroxyl group both take part in van der Waals interaction and hydrogen bonding.

SA has some advantages over most other adsorption materials due its abundance, hydrophilicity, eco-friendliness, non-toxicity and biodegradability (Karthik & Meenakshi, 2015; Yue et al., 2016). They form strong gels with trivalent and divalent cations (Mallepally et al., 2013). Nevertheless, degradation and swelling of SA are limited in water, as well as low mechanical strength. Hence, SA requires chemical modification before its utilization for the removal of some specific pollutants from wastewater (Huang & Wang, 2018). SA has been reported to be blended with materials like soil, cellulose, chitosan, polyurethane, carbon nanotube and humic acid to improve mechanical strength and adsorption capacity for the removal of pollutants from wastewater (Karthik & Meenakshi, 2015).

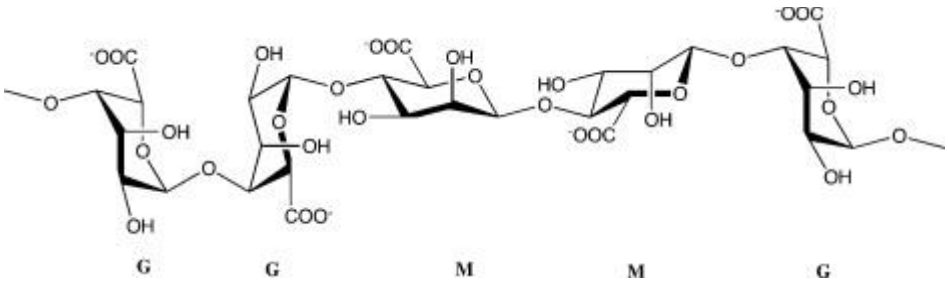

Figure 2.6: Chemical structure of alginate (Mallepally et al., 2013).

Lately, SA has been blended with polyvinyl alcohol (PVA). Owing to the outstanding properties of PVA which include a good degree of crystallinity, good chemical resistance, compact molecular packing and high-quality dispersant. This property

complement and improve the flexibility, chemical stability and durability (Yi et al., 2018).

Two or more polymers are blended to enhance and compliment the property of one or more of the polymers and also to ameliorate the cost of the product (Zhu et al., 2012). In an acidic medium (pH 4), almost all the –COOH is deprotonated to $–COO^-$, and subsequently allows for crosslinking of multivalent cations like calcium by chelation to form Semi interpenetrating network. PVA is more flexible than SA and has only one hydroxyl group in its repeating unit. Hence, SA and PVA may be combined to enhance the flexibility of SA. Blends of SA/PVA can be crosslinked chemically with glutaraldehyde (GA) (a common crosslinker) to form interpenetrating polymer network and also good compatibility in aqueous solutions (Yue et al., 2016).

So in this research, considering the mentioned properties of PVA and SA and their drawbacks, molecularly imprinted beads were fabricated using cobalt nitrate, PVA, SA for the effective adsorption of CV from aqueous solutions under varying circumstances.

Chapter 3

METHODOLOGY

3.1 Reagents and Materials

Crystal violet dye (molecular formula: $C_{25}H_{30}ClN_3$, dye% ≥ 90%, CI = 42555, MW= 407.98 g/mol, mp: 205 ^oC and λmax = 550 nm), Polyvinyl alcohol (MW = 31,000-50,000), Cobalt (II) nitrate hexahydrate {Co $(NO_3)_2.6H_2O$}(MW = 291.03 g/mol), Glutaraldehyde (GLA) (25 %) and methylene blue were purchased from Sigma Aldrich (Sigma Aldrich Co., USA). Sodium alginate (MW = 10,000 - 600,000 g/mol) was obtained from AppliChem Panreac. Sodium hydroxide (NaOH), sodium chloride ($NaCl_2$), Hydrochloric acid (HCl) were purchased as an analytical grade from Merck Co., Germany. Without any more treatments, these reagents were used.

3.2 Instrumentation

A pH meter was used to take notes of the pH values. A UV/VIS spectrophotometer (UV-1201V, Japan, Shimadu was used to take the absorbance measurements. A Vertex 70 FTIR spectrophotometer was used to obtain the infrared (IR) spectroscopy measurements. Stuart orbital shaker was used to shake the solutions.

3.3 Preparation of Cobalt-Imprinted Polymeric Co(II)-I Beads

10 mg/mL polyvinyl alcohol and sodium alginate solutions were obtained by dissolving 2500 mg of PVA and sodium alginate in distilled water (250 ml), which was stirred for 120 min at 120 ^0C for PVA and for 4 h without heat for sodium alginate at 400 rpm. The PVA was left to cool for 120 min. 100 mg/mL of Cobalt (II) nitrate

hexahydrate solution was also prepared by dissolving 10g of cobalt (II) nitrate hexahydrate crystal in 100 ml of distilled water.

The PVA solution, Sodium alginate solution and glutaraldehyde (cross-linker) were all mixed in a ratio of 5:5:1 (v/v) respectively and properly stirred. The mixture was put into a syringe and poured in a dropwise manner into the prepared aqueous cobalt (II) nitrate hexahydrate solution. This was done to obtain cobalt-imprinted polymeric beads, which were allowed to age in a conical flask for 24 h in the cobalt (II) nitrate hexahydrate solution in an incubator shaker at a 100 rpm constant speed. After which the Cobalt-imprinted beads were filtered out and the properly washed using water. The cobalt imprinted beads were put into in a 2 M HCL solution and were left in a shaker for 24 h at 100 rpm to wash out the cobalt template. The beads were then washed multiple times using distilled water. These beads were used for the batch adsorption studies.

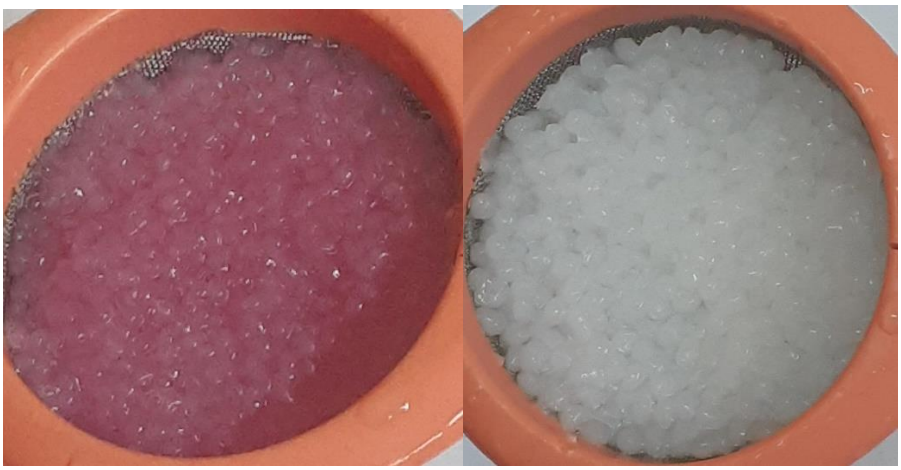

Figure 3.1: Co(II)-I beads formed before and after removal of the cobalt template.

3.4 Preparation of Adsorbates

25 mg of crystal violet dye was dissolved in 0.25 L of distilled water to obtain a 100 mg/L stock solution of crystal violet. Dilution of stock solution was done to obtain different concentrations of CV for adsorption studies. Adjustments of the dye solution was made by drops of 0.1 mol/L sodium hydroxide solution or 0.1 mol/L dilute hydrochloric acid.

3.5 Adsorbate and Adsorption Studies

20 mg/L, 25 mL volume of CV in a conical flask were used to perform the batch adsorption experiments. The solution was combined with a known mass (0.15 g) of adsorbent. A shaker was used to shake the flasks containing the solutions at 150 rpm steady speed for 20 h. Investigations were carried out on the influence of initial solution pH (2.0 - 9.0), adsorbent dose (0.15, 0.25, 0.50, 0.75, 1.00, 1.50 g), contact time (5, 10, 15, 20, 30, 60, 180, 360, 720, 1440 min) and temperature (298, 308, 318 K). The absorbance of the filtrates was noted down using.

The equation below was used to calculate the adsorption capacity of Cobalt imprinted polymer beads.

$$Q_e = \frac{(C_0 - C_t)V}{m} \qquad (3.1)$$

where:

Q_e = Adsorbed amount of specie (mg/g)

C_0 = Initial concentration of Co(II)/CV

C_t = Concentration at time t

V = Volume in aqueous phase (L)

m = Weight of adsorbent (Cobalt imprinted polymer beads)

The percentage removal efficiency of Cobalt imprinted beads was computed using the following equation:

$$R_t\ (\%) = \frac{(C_0 - C_t)}{C_0} \times 100 \qquad (3.2)$$

3.5.1 Point of zero charge (pHpzc)

The surface chemistry of the beads were investigated using the point of zero charge (pHpzc). A negative value is expected at pH values greater than the pHpzc and a positive value is expected at pH values beneath the pHpzc (Oladipo & Gazi, 2014). For pHpzc determination, 0.5 M of NaCl (25 mL) was prepared and 0.1 M dilute hydrochloric acid or 0.1 M sodium hydroxide was used to adjust the solution pH between 2.0 and 10.0. The adsorbent (0.1 g) was mixed with the solution of pH 2, 3, 4, 5, 6, 7, 8, 9 and 10, left to shake in a shaker for 20 h at 150 rpm. Thewas done to obtain the final pH value which was recorded and then plotted to obtain the pHpzc.

3.5.2 Effect of solution pH

Investigations on the influence of solution pH was carried out by varying the pH values between 2 and 9 at 20 mg/L of crystal violet and methylene blue dye concentration. 0.1 M NaOH or 0.1 M NaOH were used to adjust the pH values.

3.5.3 Effect of adsorbent dosage

Putting into consideration the best pH for the removal of crystal violet dye at pH 9, the effect of dosage was investigated using 0.15 g, 0.25 g, 0.50 g, 0.75 g, 1.00 g and 1.50 g of the cobalt imprinted polymer beads in 25 mL solution of Crystal violet dye at 20 mg/L and 298 K for 24 h.

3.5.4 Effect of initial concentration

Investigations on the effect of the initial dye concentration was carried out using 25 mL volume each of 5, 10, 15, 20, 25, 50 and 100 mg/L solutions of CV at pH 9 and a dosage of 0.15 g Co(II)-I beads at 298 K for 24 h.

3.5.5 Effect of contact time

Investigations of the contact time on removal percentage of CV onto Co(II)-I beads was carried out to ascertain the rate of removal by varying the time (5, 15, 20, 30, 60, 180, 360, 720 and 1440 min) at 20 mg/L, pH of 9, an adsorbent dosage of 0.15 g and a solution volume of 25 mL.

3.5.6 Effect of temperature

The influence of temperature was investigated by carrying out adsorption experiments under varying temperatures of 298, 308, 318 and 328 K using 25 mL of 20 mg/L of CV solution each, at pH 9, Co(II)-I dosage of 0.15 g for 6 h.

3.5.7 Effect of binary solution

Bi-solute systems (CV + MB) were prepared by mixing the varying concentrations of each dye solution (5, 10 and 20 mg/L) in a 1:1 volume ratio at pH 9, 298 K, with 0.15 g dosage of Co(II)-I beads for 3 h. The absorbance of the binary solution was taken and noted at their respective wavelengths.

3.5.8 Adsorption isotherm

Adsorption isotherm models; Freundlich, Langmuir and Dubinin - Radushkevich (D–R) (Mohanty et al., 2020) were used to determine the adsorption parameter of CV onto Co(II)-imprinted polymer beads at a constant concentration of 20mg/L.

3.5.9 Kinetic modelling

To determine and predict the adsorption equilibrium capacity and rate constants at varying temperatures, the pseudo-second-order and pseudo-first-order kinetic models were used.The pseudo-first-order kinetic model and its integrated form is described in equations (3.4) and (3.5).

- **Pseudo-first order**

$$\frac{dq}{dt} = K_1 (q_e - q_t) \quad (3.4)$$

$$\log (q_e - q_t) = \log q_e - \frac{k_1}{2.303} t \quad (3.5)$$

where:

k_1 (min^{-1}) = rate constant,

qe (mg/g) = dye adsorbed at equilibrium

q (mg/g) = dye adsorbed at time t

t (min) = time.

The k_1 was determined from the slope of plot log (qe−q) versus t.

- **Pseudo-second order**

The linear and integrated forms of pseudo-second-order kinetic model are shown in equations (3.6) and (3.7), respectively.

$$\frac{dq}{dt} = K_2 (q_e - q_t)^2 \quad (3.6)$$

$$\frac{t}{q_t} = \frac{1}{K_2 q_e^2} + \frac{1}{q_e} t \quad (3.7)$$

3.5.10 Thermodynamic studies

Thermodynamic studies on the adsorption of CV on Cobalt imprinted polymer beads was investigated by using some thermodynamic parameters like the Gibbs free energy change (ΔG°) to determine the spontaneity of the adsorption process, entropy (ΔS°) to measure the randomness or orderliness of the system, and finally enthalpy (ΔH°) to determine if the process absorbed or released heat. The thermodynamic parameters were computed using the equations below:

$$\Delta G^0 = - RTlnK_c \quad (3.9)$$

$K_c = Q_e/C_e$ (3.10)

$\Delta G^0 = \Delta H^0 - T\Delta S^0$ (3.11)

$\ln Kc = \frac{\Delta S}{R} - \frac{\Delta H}{RT}$

where:

Ce = Equilibrium concentration in solution (mg/L)

Q_e = Adsorption capacity (mg/g)

K_c = Partition coefficients of each temperature.

R = Gas constant (8.314 J/mol K)

T = Temperature in Kelvin.

The activation energy Ea for Crystal Violet adsorption onto Cobalt imprinted polymer beads was calculated by the Arrhenius equation:

$$\ln k = \ln A - \frac{E_a}{RT} \quad (3.12)$$

Activation energy is determined from the slope of plotting of ln k against 1/T.

Chapter 4

RESULTS AND DISCUSSIONS

4.1 FTIR analysis

The FTIR spectra of SA/PVA and CV-adsorbed beads are shown in Figure 4.1. The IR peaks of SA/PVA, at 3378, 2921, 1639 and 1029 cm^{-1} are indications of -OH (stretching), -CH_2 (bending), -COO- (symmetric and asymmetric stretching) and C-O-C (stretching) vibrations, respectively which is similar a study done by Yi et al. (Yi et al., 2018). The strong and broad band at 3378 cm^{-1} is due to the hydrogen bonding between the hydroxyl groups of SA and PVA (Tang et al., 2019). Upon the adsorption of CV onto SA/PVA, the peak at 1639 cm^{-1} in (a) which is due to the carboxylic group was observed to have shifted to 1584 cm^{-1} which shows clearly that carboxyl groups participated in the adsorption for CV.

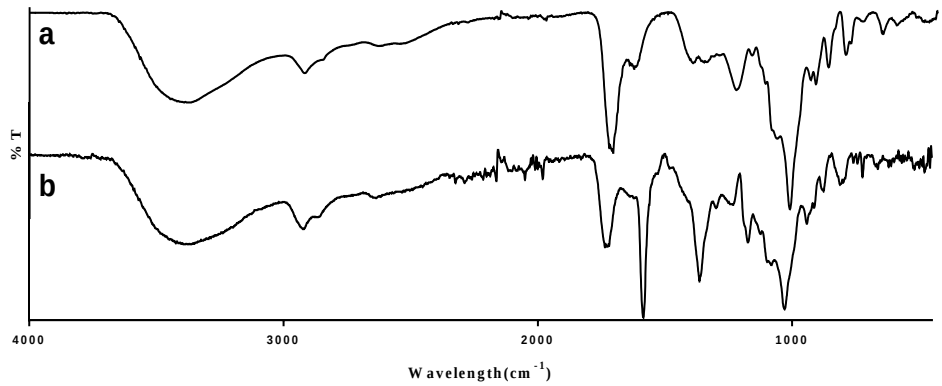

Figure 4.1: FTIR spectra; (a) Co-I polymer beads, (b) CV-adsorbed beads.

4.2 Point zero charge of Co(II)-I beads

Figure 4.2 represents the pH point zero charge (pHz) of Co(II)-I beads. The results obtained show the pHz of the beads at 3.30. This value indicates a positively charge adsorbent surface below the pHz and a negatively charge adsorbent surface above the pHz. This is in coherence with previous studies in literature as reported by Oladipo and Gazi in the removal of CV by alginate/acid-activated bentonite composite beads (Oladipo & Gazi, 2014). At low pH levels, hydroxyl and carboxyl groups get protonated which leads to electrostatic competition between the positive CV dye molecules and the positive surface of the adsorbent. Meanwhile, at higher pH levels over the pHpzc of the adsorbent, the amount of negatively charged sites for adsorption increases and the adsorption of dye is favoured by electrostatic interaction (Oladipo & Gazi, 2014).

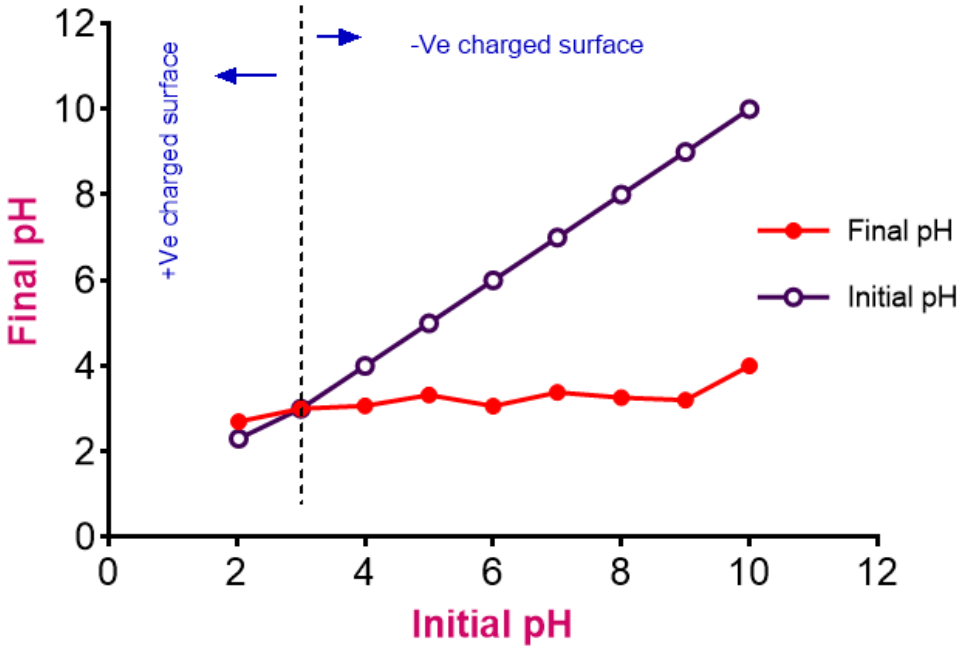

Figure 4.2: pHpzc of Co(II)-I Beads.

4.3 Effect of adsorption parameters on cobalt imprinted beads efficiency

The trends and results of the adsorption parameter are reported and discussed below. A calibration curve for Crystal violet (CV) is plotted to determine the concentrations and final concentration after adsorption by using the linear equation as seen in Figure 4.3. The average of duplicate experimental values is noted for reproducibility.

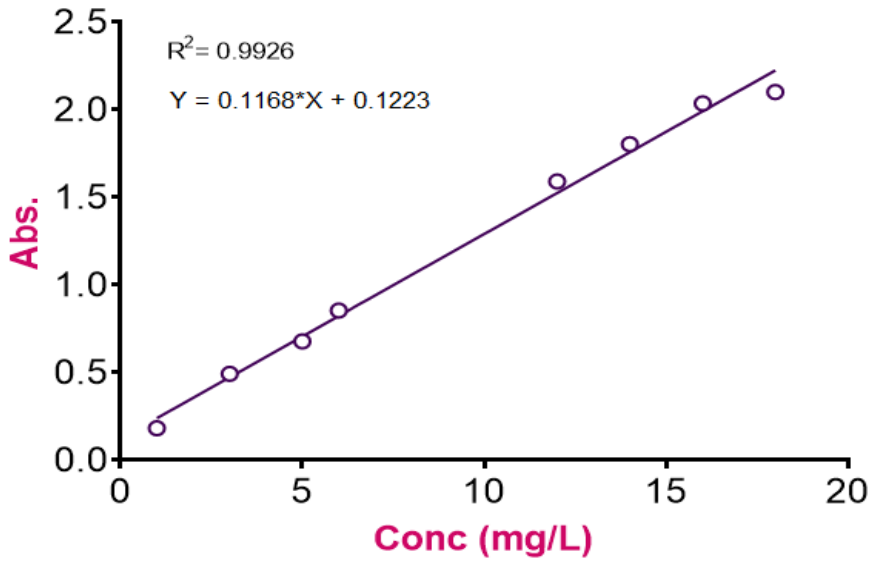

Figure 4.3: Calibration Curve for Crystal Violet.

4.3.1 Effect of solution pH

The solution pH influences the adsorption behaviour of the adsorbate in the solution. In real-life situations, the type of materials discharged into the environment (water) determines the pH of the wastewater. In this study, the efficiency of Co(II)-I beads was investigated under varying pH conditions (2 - 9) of the CV dye solution and the results are represented in Figure 4.4. From the results, maximum removal of CV dye was observed at alkaline conditions. The removal efficiency of CV dye increases with increasing pH substantially from 55 % at pH 2 to 94 % at pH 9 after 24 h at a

concentration of 20 mg/L of CV dye solution. Subsequent experiments were carried out at a pH value of 9 as a maximum removal of 94 % was obtained at this pH value. This results were similar to previous results observed for the adsorption of CV onto a newly prepared $SnFe_2O_4$ activated carbon magnetic nanocomposite and modified activated carbon/nanomagnetic iron oxide (Hamidzadeh et al., 2015; Rai et al., 2015).

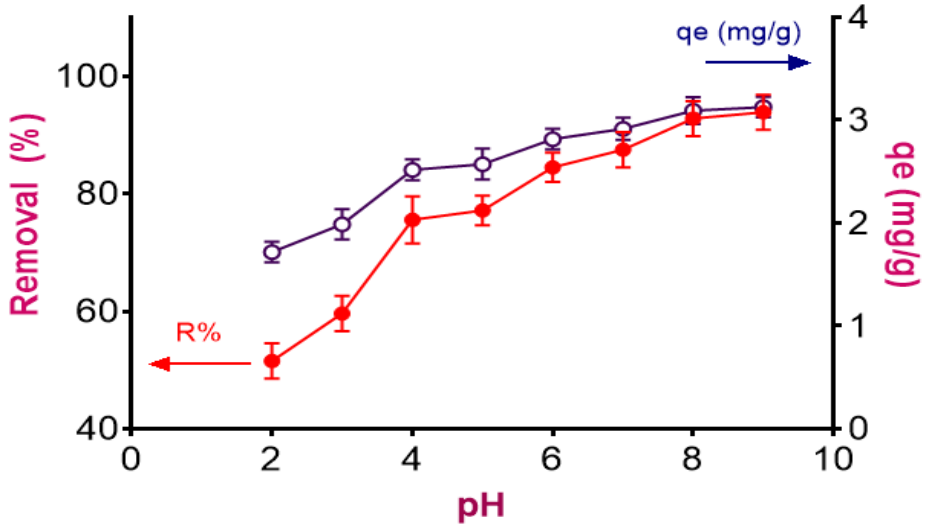

Figure 4.4: Effect of solution pH on the removal efficiency of Co(II)-I beads on CV.

The aqueous phase and the surface binding sites of the adsorbent influences the pH of the solution. Low pH values (acidic medium) are associated with the addition of protons on the adsorbent surface (Co(II)-I beads). The adsorption of the cationic CV ions decreases electrostatic repulsion which is caused by the positively charged adsorbent surface. An increased solution pH leads to a significant increment in adsorption efficiency which may be ascribed to the subsequent dehydronation of cationic groups on the surface of the adsorbent (Co(II)-I beads) and electrostatic attraction between anionic sites on the adsorbent and dye cations (Fabryanty et al., 2017).

4.3.2 Effect of adsorbent (Co(II)-I beads) dosage

The dosage of the adsorbent is a very important parameter as it significantly influences the adsorption efficiency and mechanism. The removal efficiency of CV decreased gradually from 94% to 82 % as the adsorbent dose increased from 0.15 to 1.50 g at pH 9, 20 mg/L CV concentration and 24 h as depicted in Figure 4.5. This decrease could be attributed to already filled-up binding sites due to aggregation and interaction of particles which may lead to a decreased surface area. Shoukat et al. reported similar results on the removal of crystal violet using mango bio-composites (Shoukat et al., 2017). Therefore, in subsequent experiments, the adsorbent dose was fixed at 0.15 g.

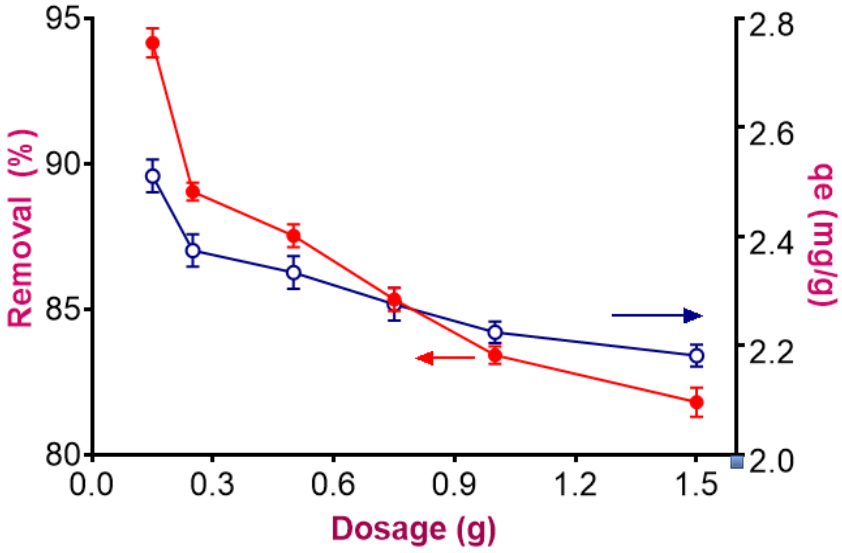

Figure 4.5: Influence of dosage of Co(II)-I beads on the removal efficiency of CV.

4.3.3 Effect of initial concentration

The adsorption efficiency was investigated by varying the concentrations of adsorbate (CV) between 5 mg/L to 100 mg/L at 0.15 g dosage of Co(II)-I beads, 298 K and at pH 9. The results are represented in Figure 4.6 and they show that the amount per unit mass of adsorbate (CV) adsorbed increased significantly as the concentration increased, while the percentage removal reduces with an increase in initial dye

concentration. At an initial concentration of 10 mg/L, 0.8 mg/g of CV was adsorbed and this amount subsequently increased to 15.9 mg/g at an initial concentration of 100 mg/L. The report verifies the reliance and proportionality of initial dye concentration and adsorption efficiency. This trend may be ascribed to the increased surface area of available sites on adsorbents as the concentration of the dye increases as well as the diffusion rate of the dye. Fewer dye cations were required for adsorption at a lower CV concentration, which increased as CV concentration increased. This trend is similar to results from the literature of the enhanced removal of CV using magnetic calcium ferrite nanoparticles (An et al., 2014).

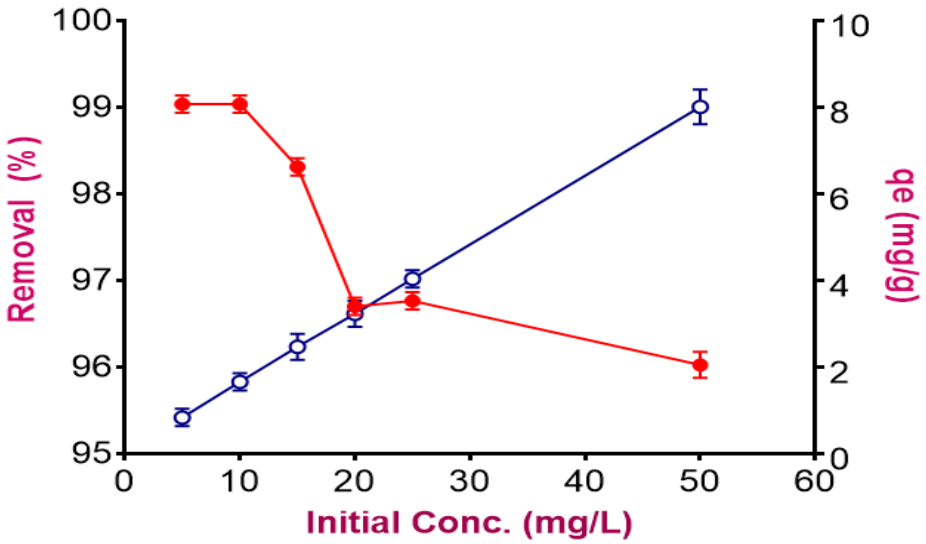

Figure 4.6: The effect of initial concentration of CV adsorption efficiency onto Co(II)-I beads.

4.3.4 Effect of Contact Time

Figure 4.7 shows the influence of contact time. The adsorbent (Co(II)-I beads) adsorbs the CV dye efficiently in the first 90 min of contact time. The availability of large surface area of the dye molecules could have led to this rate of adsorption. As the contact time is extended to about 180 min, the rate declines moderately getting to equilibrium (Chakraborty et al., 2011). A depleted binding site and a decrease in the

adsorbent surface area must have led to the decrease in the rate. 90 min was noted to be the equilibrium time for maximum dye uptake. Time-dependent change after equilibrium is not shown by the amount of adsorbed dyes. Similar results were reported according to literature on the adsorption of CV onto water hyacinth (Kulkarni et al., 2017).

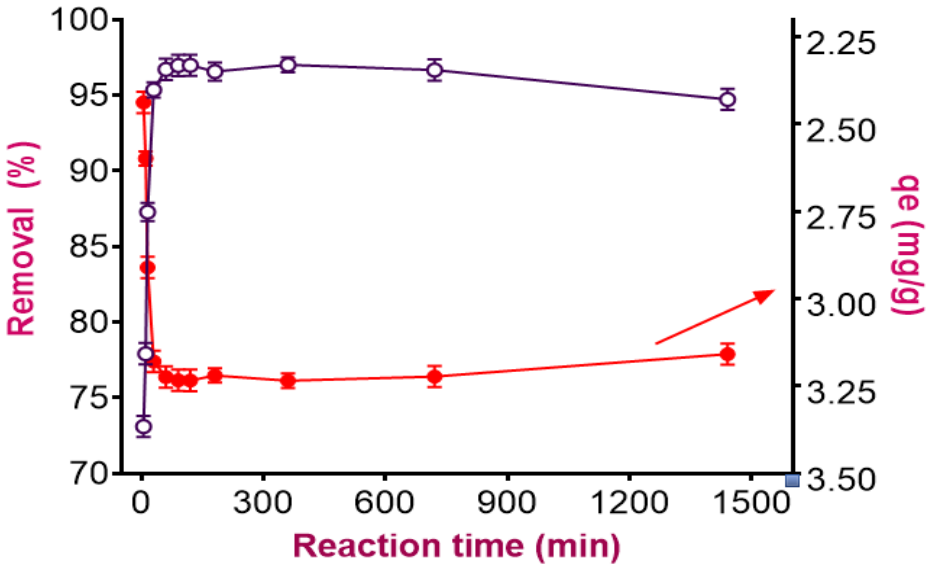

Figure 4.7: Influence of contact time of Co(II)-I beads on CV removal efficiency.

4.3.5 Effect of Binary Pollutant

The calibration curves of crystal violet and methylene blue are represented in Figure 4.8. The effect of solution pH on MB and CV are shown in Figure 4.9, which reveals that in a single system, the percentage removal of methylene blue was up to 97 %, while that of crystal violet was up to 94 %. The influence of other dye pollutants (methylene blue) is represented in Figure 4.10. Nevertheless, in the binary system, the adsorption of CV was not affected by the presence of methylene blue. Even at higher concentrations of methylene blue, adsorption of CV slightly increased. Meanwhile the adsorption of methylene blue almost remained the same. These findings are almost similar to results obtained by Liu et al. in their study on the removal of dyes from

binary systems, using a cellulose bio-adsorbent. In their study, the concentrations of methylene blue and acid blue were varied which resulted to a constant removal percentage for acid blue and an increased percentage removal for methylene blue (Lin Liu et al., 2015).

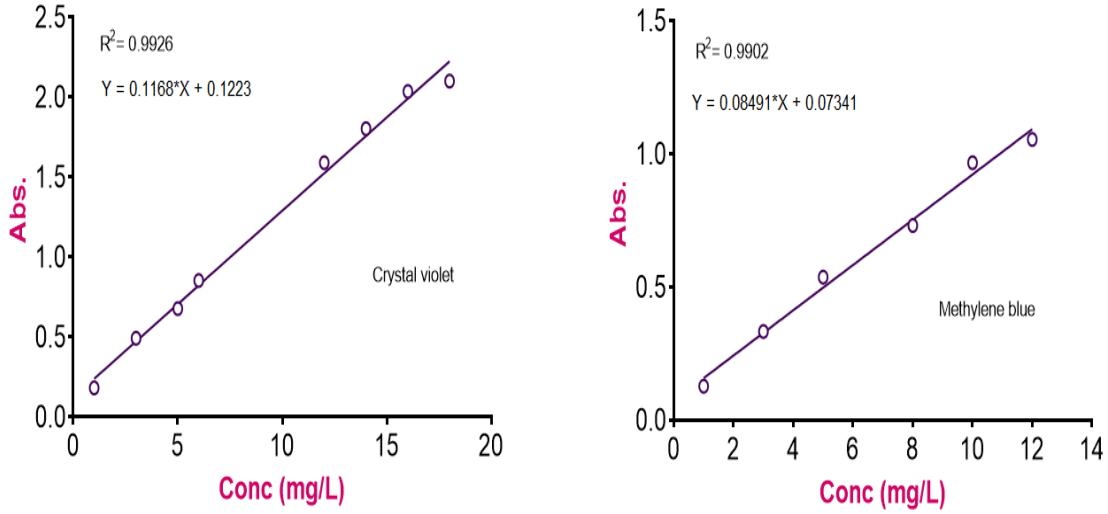

Figure 4.8: Calibration curves of Crystal violet (CV) and Methylene Blue (MB).

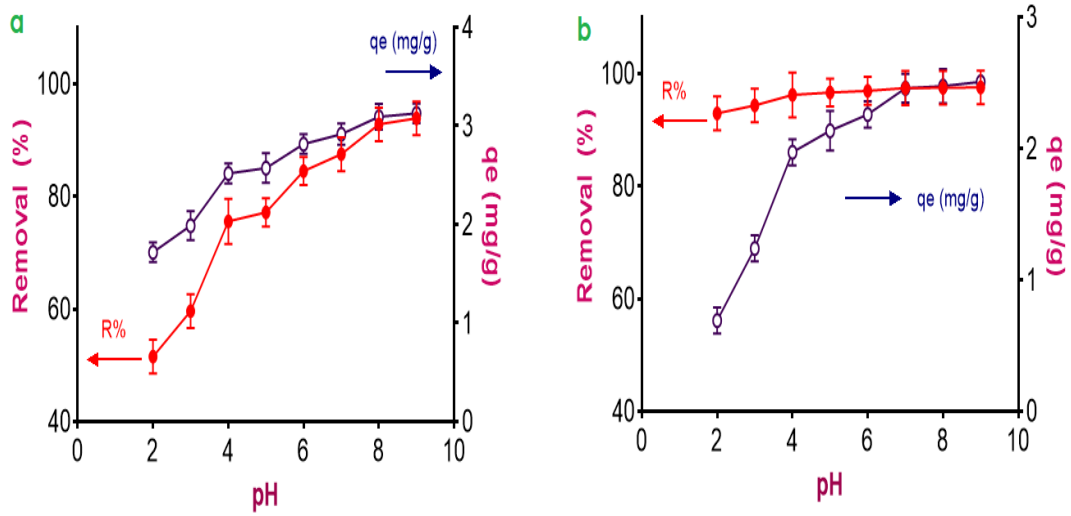

Figure 4.9: Effect of solution pH on the removal efficiency of Co(II)-I beads on (a) CV and (b) MB.

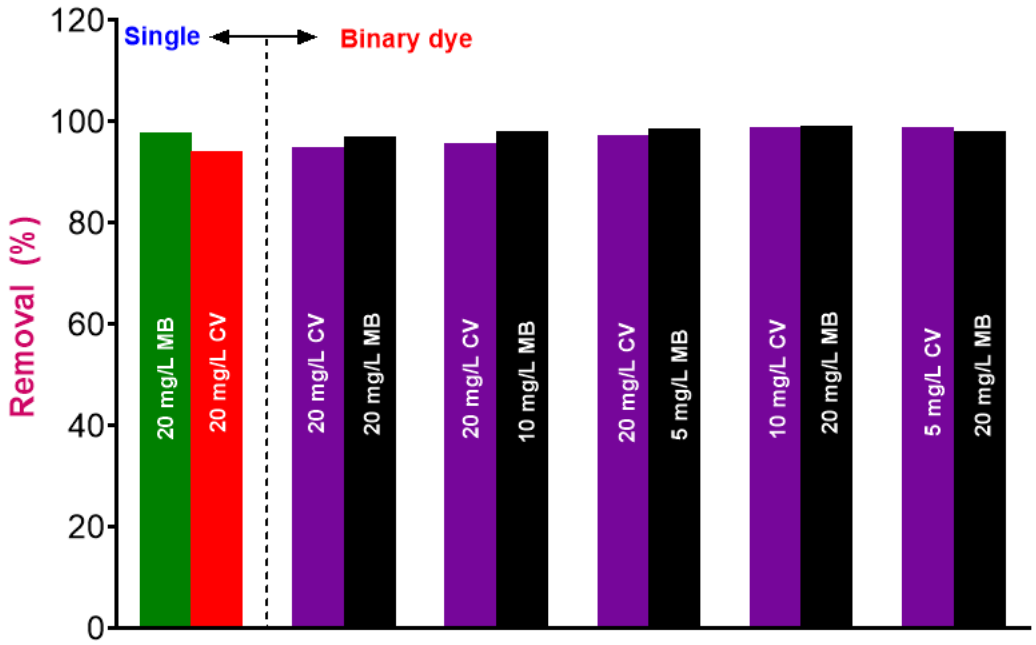

Figure 4.10: The effect of binary pollutant system: Dual removal efficiency of CV and MB.

4.3.6 Effect of Temperature

Figure 4.11 shows a decrease in the percentage removal of dye as temperature increases. This behaviour may be ascribed to the weakening of the bonds between the binding sites of the adsorbent and the dye molecules (Chakraborty et al., 2011). The trend and behavior also indicates that the adsorption of CV by Co(II)-I beads is kinetically controlled by an exothermic process. This trend also shows that the adsorption of CV onto Co(II)-I beads is coordinated by physical forces owing to the decrease in the surface activity of the adsorbent. Similar trends have been reported in literature like in the adsorption of CV using mango bio-composite (Shoukat et al., 2017).

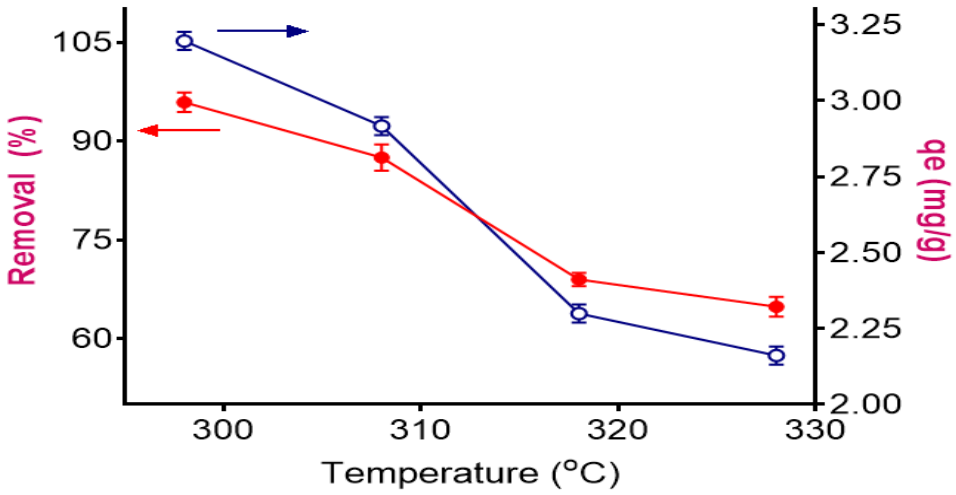

Figure 4.11: Effect of temperature.

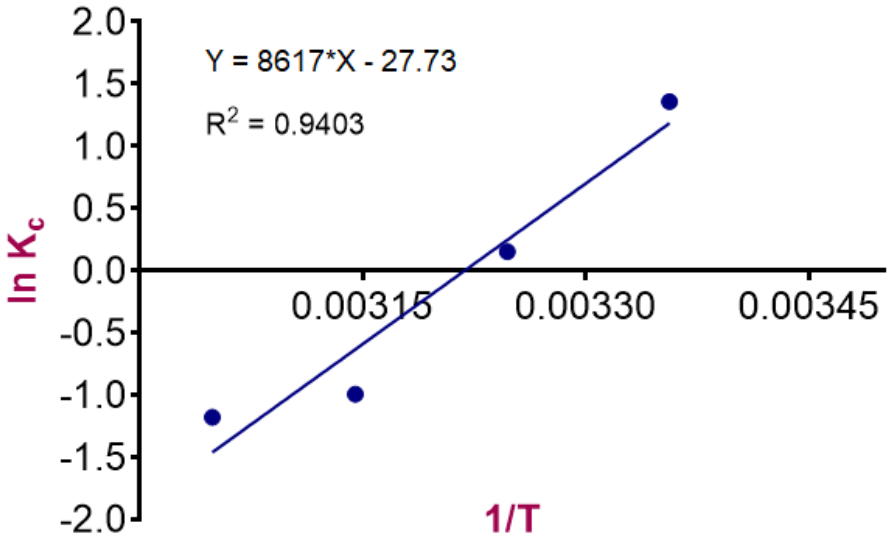

Figure 4.12: Arrhenius plot.

4.4 Adsorption thermodynamics studies

Table 4.1 gives some information on the thermodynamic parameters. The negative value of ΔH implied that the adsorption process was exothermic. Orderliness or a decrease in randomness at the solid−solution interface during CV adsorption is explained by the negative value of ΔS. The calculated E value (0.4278 kJ mol^{-1}) shows that the adsorption of CV onto Co(II)-I beads is a physisorption process as the obtained

value is lower than 8 kJ/mole. This result is consistent with the value obtained from the ΔG^o = -0.6322 − 3.9798 kJ mol^{-1}, the value of ΔG^o gives information on the type of adsorption process, indicating if it is physisorption (i.e. 20 to 0 kJ mol^{-1}) or chemisorption (i.e. 80 to 400 kJ mol^{-1}) (Oladipo and Gazi, 2014). The negative values of ΔG at 298 and 308K mean that the adsorption process was spontaneous and was favoured at low temperatures. Meanwhile, above these temperatures, the ΔG values increased and were positive indicating low adsorption capacity at high temperatures of 318K and above. These results follow the same trend with results from other study like reported by Shoukal et al. on the removal of CV using mango stone bio-composites (Shoukat et al., 2017).

Table 4.1: Thermodynamic parameters of the study at varying temperatures.

Temp (K)	K_c	Slope	Intercept	R^2	ΔH (kJ/mol)	ΔS (kJ/mol)	ΔG (kJ/mol)
298	3.8889	8617	-27.73	0.9403			-2.9382
308	1.1656				-71.657	-0.2306	-0.6322
318	0.3706						1.6738
328	0.3074						3.9798

The thermodynamic equilibrium constant Kc = qe/ce;
pH =9; Conc = 20 mg/L; Contact time = 6 h.

4.5 Adsorption kinetic Studies

Table 4.2 and Figures 4.13 and 4.14 represent the pseudo-first order and second-order kinetic models. From the table, it can be observed that the adsorption process follows the pseudo-second order kinetic model as it has the highest correlation value of (R^2 = 0.999). The results are similar to the results obtained from similar studies like the

adsorption of CV by modified activated carbon and nano-magnetic iron oxide (Hamidzadeh et al., 2015).

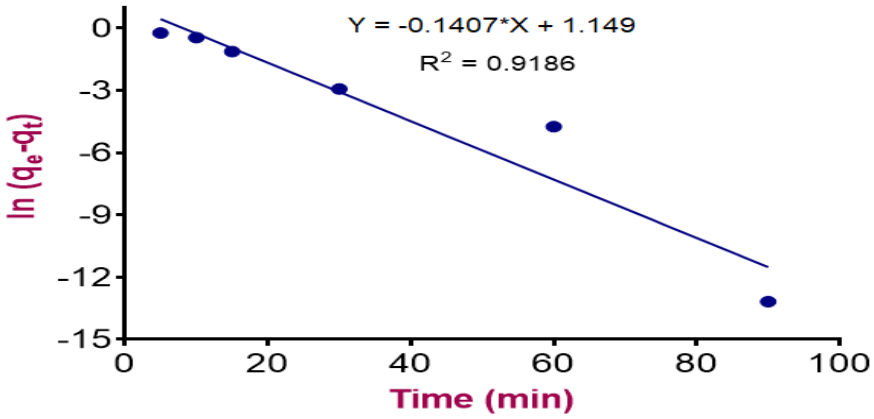

Figure 4.13: Pseudo-first order plot of CV adsorption onto Co(II)-I beads.

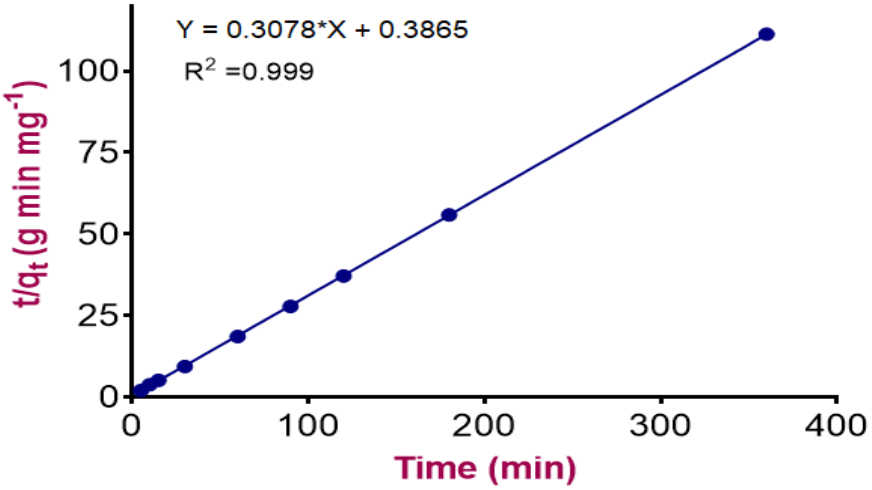

Figure 4.14: Pseudo-second order plot of CV adsorption onto Co(II)-I beads.

Table 4.2: The pseudo-first and pseudo-second kinetic constants and coefficients of determination for adsorption of CV+ by Co(II)-I beads (T = 25 °C, pH = 9.0).

Kinetic models	Parameters	Values
Pseudo-first-order	K_1 (min^{-1})	1.149
	q_e (mg/g)	0.1407
	R^2	0.9186
Pseudo-second-order	K_2 (min^{-1})	0.3865
	q_e (mg/g)	0.3078
	R^2	0.999

4.6 Adsorption Isotherms

The R^2 values and other parameters attained from the plots of and Dubinin - Radushkevich (D–R) (lnqe versus ε^2), Freundlich (ln qe versus ln Ce) and Langmuir (1/qe versus 1/Ce), and are noted down in Table 4.2. The isotherm models are represented in Figures 4.15, 4.16 and 4.17. From table 4.2. It is observed that the Langmuir isotherm model best describes the adsorption process of CV onto Co(II)-I beads with a better correlation value of (R^2 = 0.9757) closer to unity than that of Freundlich (R^2 = 0.9037) and Dubinin -Radushkevich (R^2 = 0.8749). The results indicate that the adsorption process is homogeneous. Also, the value of n indicates a successful adsorption of CV onto Co(II)-I beads. This result is similar to a study on the adsorption of CV onto mango stone biocomposite (Shoukat et al., 2017).

For the Freuindlich isotherm model, the value of the adsorption intensity (n) obtained from this study was 1.08 which is greater than 1 and indicates high affinity of the adsorbate CV towards the Co(II)-I beads. The maximum adsorptive capacity K_F

obtained was 13.87 CV/g Co(II)-I beads. In the case of the Langmuir isotherm model, the R_L value obtained from this study was 0.067 which is less than 1, which means that adsorption of CV onto Co(II)-I beads was favourable. The maximum adsorption capacity Q_{max} obtained was 25.21 mg/g. For Dubinin - Radushkevich (D–R) isotherm, the calculated value of E obtained from the study obtained from this study was 0.4278 kJ mol^{-1} which denotes that the CV adsorption onto Co(II)-I beads is a Physisorption process as the obtained value is lower than 8 kJ/mole (Oladipo & Gazi, 2014).

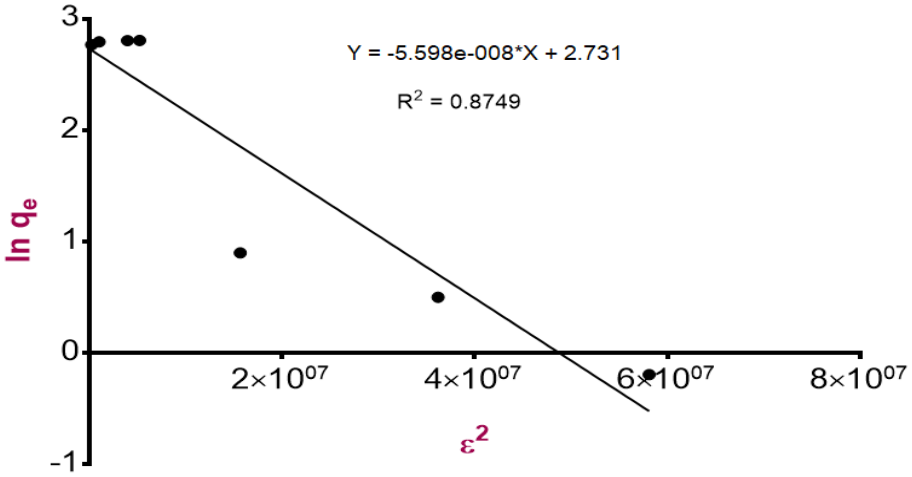

Figure 4.15: Dubinin - Radushkevich (D–R) isotherm.

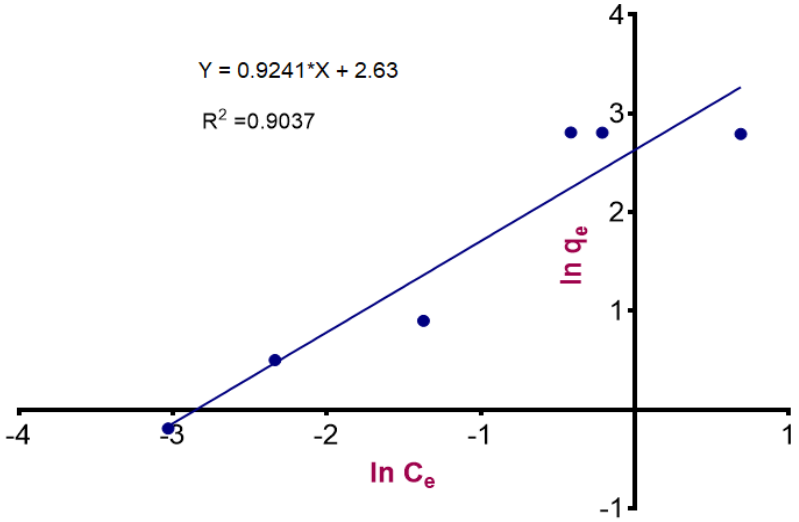

Figure 4.16: Freudlich isotherm model.

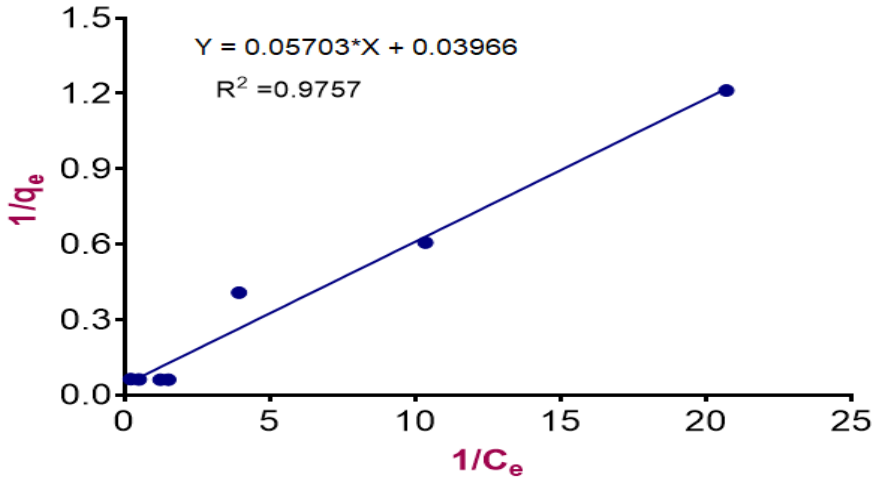

Figure 4.17: Langmuir isotherm model.

Table 4.3: Adsorption isotherm parameters for the adsorption of CV onto Co(II)-I beads.

Isotherm models	Parameters	Values
Langmuir	Qm (mg/g)	25.21
	b (L/mg)	0.696
	R_L	0.067
	R^2	0.976
Dubinin - Radushkevich	K_T (L/g)	0.0314
	E (kJ/mol)	0.4278
	R^2	0.8749
Freundlich	K_f (L/mg)	13.87
	n	1.08
	R^2	0.907

Table 4.4: Comparison of some adsorption isotherm parameters for the adsorption of CV from other studies and this study.

		Langmuir Isotherm					**Freundlich isotherm**			**Ref**
Dye	C_o (mg/L)	Temp. (K)	Q_{max} (mg/g)	b (L/mg)	R^2	R_L	*n*	k_f	R^2	
CV	20	298	25.21	0.696	0.976	0.067	1.08	13.87	0.904	**This study**
	20	298	8.361	0.34	0.977	0.13	3.56	3.387	0.985	Mohanty et al. 2020
	100	288	480.21	$152x10^3$	0.950	$6.6x10^{-3}$	9.86	62.35	0.920	Oladipo & Gazi, 2014
	5	293	44.7	0.4	0.995	0.333	1.90	12.7	0.969	(Hamidzadeh et al., 2015)
	500	300	322.58	0.688	0.9644	2.9×10^{-3}	3.792	121.63	0.9394	(Kulkarni et al., 2017)
	50	306	500	26	0.94	7.6×10^{-4}	6.098	1.007	0.520	(Shoukat et al., 2017)
	300	303	127.2	0.02	0.99	0.1428	1.734	5.999	0.991	(Fabryanty et al., 2017)
	25	303	105.26	3.6×10^{-4}	0.997	0.991	1.38	104.71	0.997	(Rai et al., 2015)

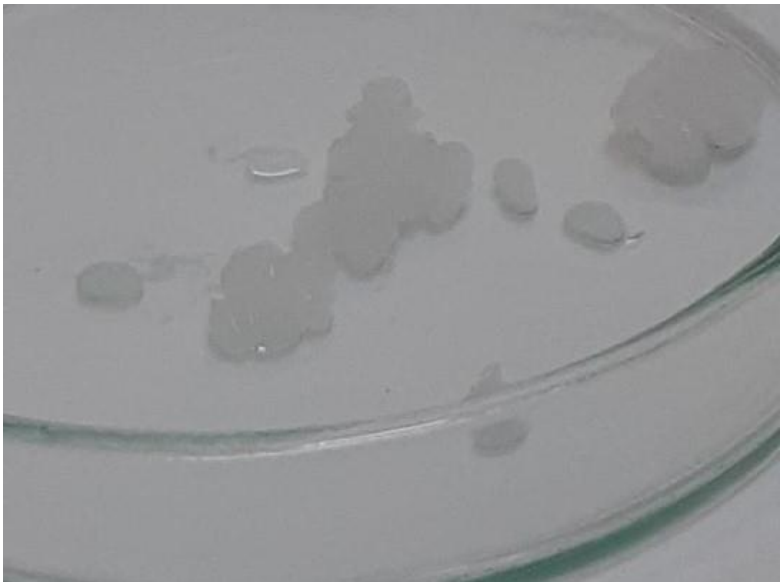

Figure 4.18: Co(II)-I beads before adsorption.

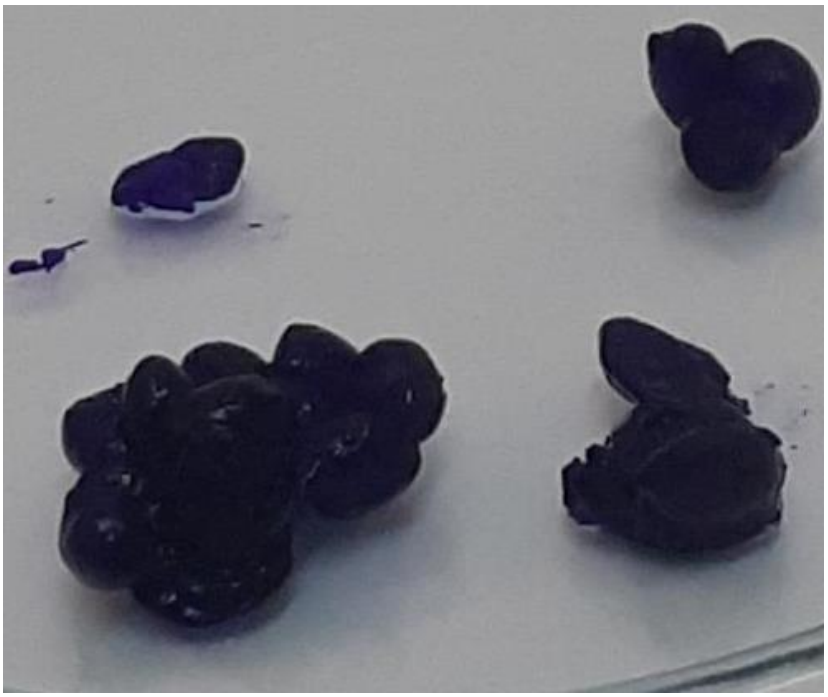

Figure 4.19: Co(II)-I beads after adsorption.

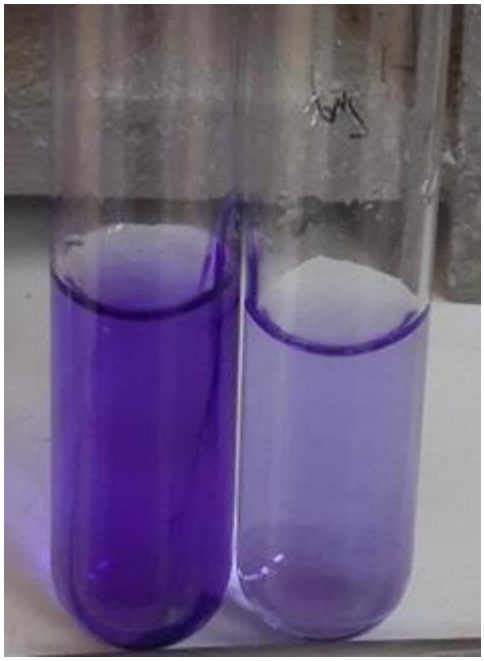

Figure 4.20: Crystal violet dye solution (20 mg/L) before and after adsorption.

Chapter 5

CONCLUSION

Cobalt imprinted polymer beads (Co(II)-I beads) were synthesized by a simple method as described in the third chapter. The surface characteristics of the prepared adsorbent and the adsorption of crystal violet dye onto Co(II)-I beads was explained and confirmed by the FTIR methods. Here is a summary of the results and trends observed:

1. A value of 3.30 was established as the point zero charge of the adsorbent
2. The efficiency of the prepared adsorbent for the removal of crystal violet dye was influenced by the various adsorption parameters like the adsorbent dosage, solution pH value, contact time, initial dye concentration, and temperature.
3. Maximum removal percentage (94 %) of CV was obtained at pH 9.
4. The removal efficiency reduced substantially as the adsorbent dosage increased from 150 mg to 1500 mg; hence, 1500 mg was selected as the optimum dosage for subsequent study.
5. An increase in the removal efficiency of Co(II)-I beads was observed with the contact time until an equilibrium was attained at 90 min.
6. The removal efficiency of Co(II)-I beads was observed to decrease with an increase in temperature which depicted an exothermic adsorption process. An increased initial dye concentration was observed to decrease the removal efficiency. The adsorption thermodynamic parameters describe the adsorption process to be spontaneous, feasible, exothermic and physical. The Langmuir isotherm model was the best fit for describing the adsorption process.

However, further studies will be carried out on a suitable solvent for desorption and regeneration studies.

REFERENCES

Al-Senani, G. M., & Al-Kadhi, N. S. (2020). Studies on Adsorption of Fluorescein Dye from Aqueous Solutions Using Wild Herbs. *International Journal of Analytical Chemistry*, *2020*. https://doi.org/10.1155/2020/8019274

Aljeboree, A. M., Alshirifi, A. N., & Alkaim, A. F. (2017). Kinetics and equilibrium study for the adsorption of textile dyes on coconut shell activated carbon. *Arabian Journal of Chemistry*, *10*, S3381–S3393. https://doi.org/10.1016/j.arabjc.2014.01.020

An, S., Liu, X., Yang, L., & Zhang, L. (2014). Chemical Engineering Research and Design Enhancement removal of crystal violet dye using magnetic calcium ferrite nanoparticle : Study in single- and binary-solute systems. *Chemical Engineering Research and Design*, *94*(October), 726–735. https://doi.org/10.1016/j.cherd.2014.10.013

Ayawei, N., Ebelegi, A. N., & Wankasi, D. (2017). Modelling and Interpretation of Adsorption Isotherms. *Journal of Chemistry*, *2017*. https://doi.org/10.1155/2017/3039817

Benkhaya, S., Harfi, S. El, & Harfi, A. El. (2018). *Classifications , properties and applications of textile dyes : A review*. *January 2017*.

Benkhaya, S., Souad, M., & Harfi, A. El. (2020). A review on classifications , recent synthesis and applications of textile dyes. *Inorganic Chemistry Communications*,

115(January), 107891. https://doi.org/10.1016/j.inoche.2020.107891

Biswas, T. K., Yusoff, M. M., Sarjadi, M. S., Arshad, E., Musta, B., & Rahman, L. (2019). Ion-imprinted polymer for selective separation of cobalt , cadmium and lead ions from aqueous media. *Separation Science and Technology*, *0*(0), 1–10. https://doi.org/10.1080/01496395.2019.1575418

Brillas, E., & Martínez-Huitle, C. A. (2015). Decontamination of wastewaters containing synthetic organic dyes by electrochemical methods. An updated review. *Applied Catalysis B: Environmental*, *166–167*, 603–643. https://doi.org/10.1016/j.apcatb.2014.11.016

Chakraborty, S., Chowdhury, S., & Das Saha, P. (2011). Adsorption of Crystal Violet from aqueous solution onto NaOH-modified rice husk. *Carbohydrate Polymers*, *86*(4), 1533–1541. https://doi.org/10.1016/j.carbpol.2011.06.058

Chen, J. H., Li, G. P., Liu, Q. L., Ni, J. C., Wu, W. B., & Lin, J. M. (2010). Cr(III) ionic imprinted polyvinyl alcohol/sodium alginate (PVA/SA) porous composite membranes for selective adsorption of Cr(III) ions. *Chemical Engineering Journal*, *165*(2), 465–473. https://doi.org/10.1016/j.cej.2010.09.034

D'Antoni, B. M., Iracà, F., & Romero, M. (2017). Current treatment technologies and practical approaches on textile wastewater Dyes Removal. *Panta Rei Srl-Water Solutions, April 2017*, 1–10.

De Gisi, S., Lofrano, G., Grassi, M., & Notarnicola, M. (2016). Characteristics and

adsorption capacities of low-cost sorbents for wastewater treatment: A review. *Sustainable Materials and Technologies*, *9*, 10–40. https://doi.org/10.1016/j.susmat.2016.06.002

Fabryanty, R., Valencia, C., Edi, F., & Nyoo, J. (2017). *Journal of Environmental Chemical Engineering Removal of crystal violet dye by adsorption using bentonite – alginate composite*. *5*(July), 5677–5687. https://doi.org/10.1016/j.jece.2017.10.057

Guo, Y., Zhao, J., Zhang, H., Yang, S., Qi, J., Wang, Z., & Xu, H. (2005). Use of rice husk-based porous carbon for adsorption of Rhodamine B from aqueous solutions. *Dyes and Pigments*, *66*(2), 123–128. https://doi.org/10.1016/j.dyepig.2004.09.014

Hamidzadeh, S., Torabbeigi, M., & Shahtaheri, S. J. (2015). Removal of crystal violet from water by magnetically modified activated carbon and nanomagnetic iron oxide. *Journal of Environmental Health Science & Engineering*, *13*(8), 1–7. https://doi.org/10.1186/s40201-015-0156-4

Huang, D. L., Wang, R. Z., Liu, Y. G., Zeng, G. M., Lai, C., Xu, P., Lu, B. A., Xu, J. J., Wang, C., & Huang, C. (2014). Application of molecularly imprinted polymers in wastewater treatment: a review. *Environmental Science and Pollution Research*, *22*(2), 963–977. https://doi.org/10.1007/s11356-014-3599-8

Huang, Y., & Wang, Z. (2018). Preparation of composite aerogels based on sodium alginate, and its application in removal of Pb2+and Cu2+from water.

International Journal of Biological Macromolecules, *107*(PartA), 741–747. https://doi.org/10.1016/j.ijbiomac.2017.09.057

Kang, R., Qiu, L., Fang, L., Yu, R., Chen, Y., Lu, X., & Luo, X. (2016). A novel magnetic and hydrophilic ion-imprinted polymer as a selective sorbent for the removal of cobalt ions from industrial wastewater. *Journal of Environmental Chemical Engineering*, *4*(2), 2268–2277. https://doi.org/10.1016/j.jece.2016.04.010

Karimi, S., & Tavakkoli, M. (2019). A comprehensive review of the adsorption mechanisms and factors influencing the adsorption process from the perspective of bioethanol dehydration. *Renewable and Sustainable Energy Reviews*, *107*(March), 535–553. https://doi.org/10.1016/j.rser.2019.03.025

Karthik, R., & Meenakshi, S. (2015). Removal of Cr(VI) ions by adsorption onto sodium alginate-polyaniline nanofibers. *International Journal of Biological Macromolecules*, *72*, 711–717. https://doi.org/10.1016/j.ijbiomac.2014.09.023

Kulkarni, M. R., Revanth, T., Acharya, A., & Bhat, P. (2017). Removal of Crystal Violet dye from aqueous solution using water hyacinth : Equilibrium , kinetics and thermodynamics study. *Resource-Efficient Technologies*, *3*(1), 71–77. https://doi.org/10.1016/j.reffit.2017.01.009

Li, W., Mu, B., & Yang, Y. (2019). Feasibility of industrial-scale treatment of dye wastewater via bio-adsorption technology. *Bioresource Technology*, *277*(January), 157–170. https://doi.org/10.1016/j.biortech.2019.01.002

Lin, D., Wu, F., Hu, Y., Zhang, T., Liu, C., Hu, Q., Hu, Y., Xue, Z., Han, H., & Ko, T. H. (2020). Adsorption of Dye by Waste Black Tea Powder: Parameters, Kinetic, Equilibrium, and Thermodynamic Studies. *Journal of Chemistry*, *2020*. https://doi.org/10.1155/2020/5431046

Liu, Lin, Gao, Z. Y., Su, X. P., Chen, X., Jiang, L., & Yao, J. M. (2015). Adsorption removal of dyes from single and binary solutions using a cellulose-based bioadsorbent. *ACS Sustainable Chemistry and Engineering*, *3*(3), 432–442. https://doi.org/10.1021/sc500848m

Liu, Lingling, Luo, X., Ding, L., & Luo, S. (2019). 4 - Application of Nanotechnology in the Removal of Heavy Metal From Water. In *Nanomaterials for the Removal of Pollutants and Resource Reutilization*. Elsevier Inc. https://doi.org/10.1016/B978-0-12-814837-2.00004-4

Liu, W., Zhang, M., Liu, X., Zhang, H., Jiao, J., Zhu, H., Zhou, Z., & Ren, Z. (2020). *Preparation of Surface Ion-Imprinted Materials Based on Modi fi ed Chitosan for Highly Selective Recognition and Adsorption of Nickel Ions in Aqueous Solutions*. https://doi.org/10.1021/acs.iecr.9b04755

Mallepally, R. R., Bernard, I., Marin, M. A., Ward, K. R., & McHugh, M. A. (2013). Superabsorbent alginate aerogels. *Journal of Supercritical Fluids*, *79*, 202–208. https://doi.org/10.1016/j.supflu.2012.11.024

Mohanty, S., Moulick, S., & Maji, S. K. (2020). Adsorption/photodegradation of crystal violet (basic dye) from aqueous solution by hydrothermally synthesized titanate

nanotube (TNT). *Journal of Water Process Engineering*, *37*(February), 101428. https://doi.org/10.1016/j.jwpe.2020.101428

Oladipo, A. A., & Gazi, M. (2014). Journal of Water Process Engineering Enhanced removal of crystal violet by low cost alginate / acid activated bentonite composite beads : Optimization and modelling using non-linear regression technique. *Journal of Water Process Engineering*, *2*, 43–52. https://doi.org/10.1016/j.jwpe.2014.04.007

Oladipo, A. A., & Gazi, M. (2015). Journal of the Taiwan Institute of Chemical Engineers Microwaves initiated synthesis of activated carbon-based composite hydrogel for simultaneous removal of copper (II) ions and direct red 80 dye : A multi-component adsorption system. *Journal of the Taiwan Institute of Chemical Engineers*, *47*, 125–136. https://doi.org/10.1016/j.jtice.2014.09.027

Parlayici, Ş. (2019). Alginate-coated perlite beads for the efficient removal of methylene blue, malachite green, and methyl violet from aqueous solutions: kinetic, thermodynamic, and equilibrium studies. *Journal of Analytical Science and Technology*, *10*(1). https://doi.org/10.1186/s40543-019-0165-5

Piccin, J. S., Dotto, G. L., & Pinto, L. A. A. (2011). Adsorption isotherms and thermochemical data of FDandC RED N° 40 Binding by chitosan. *Brazilian Journal of Chemical Engineering*, *28*(2), 295–304. https://doi.org/10.1590/S0104-66322011000200014

Rai, P., Gautam, R. K., Banerjee, S., Rawat, V., & Chattopadhyaya, M. C. (2015).

Synthesis and characterization of a novel SnFe2O4@activated carbon magnetic nanocomposite and its effectiveness in the removal of crystal violet from aqueous solution. *Journal of Environmental Chemical Engineering*, *3*(4), 2281–2291. https://doi.org/10.1016/j.jece.2015.08.017

Rápó, E., Aradi, L. E., Szabó, Á., Posta, K., Szép, R., & Tonk, S. (2020). Adsorption of Remazol Brilliant Violet-5R Textile Dye from Aqueous Solutions by Using Eggshell Waste Biosorbent. *Scientific Reports*, *10*(1), 1–12. https://doi.org/10.1038/s41598-020-65334-0

Saraji, M., & Yousefi, H. (2009). Selective solid-phase extraction of Ni(II) by an ion-imprinted polymer from water samples. *Journal of Hazardous Materials*, *167*(1–3), 1152–1157. https://doi.org/10.1016/j.jhazmat.2009.01.111

Şen, F., Demirbaş, Ö., Çalımlı, M. H., Aygün, A., Alma, M. H., & Nas, M. S. (2018). The dye removal from aqueous solution using polymer composite films. *Applied Water Science*, *8*(7), 1–9. https://doi.org/10.1007/s13201-018-0856-x

Shoukat, S., Nawaz, H., Iqbal, M., & Noreen, S. (2017). Microporous and Mesoporous Materials Mango stone biocomposite preparation and application for crystal violet adsorption : A mechanistic study. *Microporous and Mesoporous Materials*, *239*, 180–189. https://doi.org/10.1016/j.micromeso.2016.10.004

Sikaily, A. El, Khaled, A., & El Nemr, A. (2012). Textile dyes xenobiotic and their harmful effect. In *Non-Conventional Textile Waste Water Treatment* (Issue January).

Tang, Y., Lan, X., Liang, C., Zhong, Z., Xie, R., Zhou, Y., Miao, X., Wang, H., & Wang, W. (2019). Honey loaded alginate / PVA nano fi brous membrane as potential bioactive wound dressing. *Carbohydrate Polymers*, *219*(April), 113–120. https://doi.org/10.1016/j.carbpol.2019.05.004

Yadav, S., Asthana, A., Chakraborty, R., & Jain, B. (2020). *Cationic Dye Removal Using Novel Magnetic / Activated Charcoal / β - Cyclodextrin / Alginate Polymer Nanocomposite*. 1–20.

Yi, X., Sun, F., Han, Z., Han, F., He, J., Ou, M., Gu, J., & Xu, X. (2018). Graphene oxide encapsulated polyvinyl alcohol/sodium alginate hydrogel microspheres for Cu (II) and U (VI) removal. *Ecotoxicology and Environmental Safety*, *158*(May), 309–318. https://doi.org/10.1016/j.ecoenv.2018.04.039

Yue, Y., Han, J., Han, G., French, A. D., Qi, Y., & Wu, Q. (2016). Cellulose nanofibers reinforced sodium alginate-polyvinyl alcohol hydrogels: Core-shell structure formation and property characterization. *Carbohydrate Polymers*, *147*, 155–164. https://doi.org/10.1016/j.carbpol.2016.04.005

Zhu, H. Y., Fu, Y. Q., Jiang, R., Yao, J., Xiao, L., & Zeng, G. M. (2012). Novel magnetic chitosan/poly(vinyl alcohol) hydrogel beads: Preparation, characterization and application for adsorption of dye from aqueous solution. *Bioresource Technology*, *105*, 24–30. https://doi.org/10.1016/j.biortech.2011.11.057

Zhu, Y., Hu, J., & Wang, J. (2014). Removal of Co2+ from radioactive wastewater by polyvinyl alcohol (PVA)/chitosan magnetic composite. *Progress in Nuclear*

Energy, *71*, 172–178. https://doi.org/10.1016/j.pnucene.2013.12.005